



**HAL**  
open science

**Pedological (micromorphological and chemical) investigation in an archaeological site of the Early Bronze Age: the case study of Palma Campania (southern Italy): Soil properties of the last 9000 years in a plain close to Vesuvius**

Simona Vingiani, Luciana Minieri, Claude Albore Livadie, Fabio Terribile

► **To cite this version:**

Simona Vingiani, Luciana Minieri, Claude Albore Livadie, Fabio Terribile. Pedological (micromorphological and chemical) investigation in an archaeological site of the Early Bronze Age: the case study of Palma Campania (southern Italy): Soil properties of the last 9000 years in a plain close to Vesuvius. 2016. hal-01479488

**HAL Id: hal-01479488**

**<https://hal.science/hal-01479488>**

Preprint submitted on 28 Feb 2017

**HAL** is a multi-disciplinary open access archive for the deposit and dissemination of scientific research documents, whether they are published or not. The documents may come from teaching and research institutions in France or abroad, or from public or private research centers.

L'archive ouverte pluridisciplinaire **HAL**, est destinée au dépôt et à la diffusion de documents scientifiques de niveau recherche, publiés ou non, émanant des établissements d'enseignement et de recherche français ou étrangers, des laboratoires publics ou privés.



**Pedological (micromorphological and chemical)  
investigation in an archaeological site of the Early Bronze  
Age: the case study of Palma Campania (southern Italy).**

Journal:	<i>Geoarchaeology</i>
Manuscript ID	GEO-16-010
Wiley - Manuscript type:	Research Article
Date Submitted by the Author:	01-Feb-2016
Complete List of Authors:	Vingiani, Simona; Universita degli Studi di Napoli Federico II, Department of Agricultural Sciences; Universita degli Studi di Napoli Federico II, CRISP - Interdepartmental Research Center on the Earth Critical Zone Minieri, Luciana; Universita degli Studi di Napoli Federico II, Department of Agricultural Sciences Albore Livadie, Claude; CNRS, Centre Camille Jullian Di Vito, Mauro Antonio; Istituto Nazionale di Geofisica e Vulcanologia - Osservatorio Vesuviano, Via Diocleziano, 328 Terribile, Fabio; University of Naples Federico II, Department of Agricultural Sciences; University of Naples Federico II, CRISP - Interdepartmental Research Center on the Earth Critical Zone
Keywords:	soil chronosequence, micromorphological features, Early Bronze Age, soil fertility, climatic indicators

SCHOLARONE™  
Manuscripts

1  
2  
3 1 **Pedological (micromorphological and chemical) investigation in an archaeological site of the**  
4  
5 2 **Early Bronze Age: the case study of Palma Campania (southern Italy).**  
6  
7 3  
8

9 4 Running head: soil properties of the last 9000 years in a plain close to Vesuvius  
10  
11 5

12  
13 6 Vingiani Simona<sup>ab\*</sup>, Minieri Luciana<sup>a</sup>, Albore Livadie Claude<sup>c</sup>, Mauro A. Di Vito<sup>d</sup>, Terribile  
14  
15 Fabio<sup>ab</sup>  
16  
17  
18 8

19  
20 9 <sup>a</sup>Department of Agricultural Sciences, University of Naples Federico II – Via Università 100, 80055  
21  
22 Portici (NA) - Italy  
23  
24

25 11 <sup>b</sup>CRISP - Interdepartmental Research Center on the Earth Critical Zone, University of Naples  
26  
27 Federico II - Via Università 100, 80055 - Portici (NA) - Italy  
28

29 13 <sup>c</sup>CNRS, Centre Camille Jullian – Aix-en-Provence – France  
30

31 14 <sup>d</sup>Istituto Nazionale di Geofisica e Vulcanologia – sezione di Napoli Osservatorio Vesuviano, Via  
32  
33 Diocleziano, 328 – Napoli - Italy  
34  
35

36 16  
37  
38 17 \*corresponding author  
39  
40  
41 18

42  
43 19 **Keywords:** soil chronosequence, micromorphological features, Early Bronze Age, soil fertility,  
44  
45 climatic indicators  
46  
47 21

48  
49 22 **ABSTRACT**




50  
51 23 Archaeological records from excavations of the last forty years in the Campania region (southern  
52  
53 Italy) attest to an intense human occupation from the Early Bronze Age (EBA) until the present day.  
54  
55

56 25 A soil study, aimed to the better understanding of fertility, use and environmental conditions of the  
57  
58 26 land where these past communities lived, was carried out at Palma Campania (Naples) over an  
59  
60

1  
2  
3 27 Eneolithic to Modern Age chronosequence and an EBA paleosurface. The results shown that soils i)  
4  
5 28 were Andosols, ii) differ markedly in terms of depth, degree of andic properties and chemical  
6  
7 29 fertility, iii) had micromorphological features (e.g. silty coatings, laminar features, iron  
8  
9 30 segregations, weathering rims etc.) indicating specific weathering environments. The comparison of  
10  
11 31 the estimated pedogenetic times (EPT) and selected soil properties (Al and Fe ammonium oxalate  
12  
13 32 extractable forms and organic matter) with climate evaluations from the literature highlighted a  
14  
15 33 marked relationship between these properties and the humidity/aridity of the environment.  
16  
17 34 Regarding the EBA paleo-surface, the organic-phosphorous content and the organic matter of some  
18  
19 35 areas resulted consistent with both archaeological contexts and reconstructed agricultural uses  
20  
21 36 (animal pasturing and crop cultivation), whereas the specific micromorphological pedo-features and  
22  
23 37 chemical properties strongly suggest anthropic genesis for an ancient micro-topography of  
24  
25  
26  
27 38 undefined origin.  
28  
29  
30  
31

## 32 40 1. INTRODUCTION

33  
34 41 Recent archaeological and volcanological studies carried out in the Campania region (southern  
35  
36 42 Italy) have shown that the activity of the Quaternary volcanic edifices (i.e. Vesuvius,  
37  
38 43 Roccamonfina, Campi Flegrei and Isle of Ischia) along the Tyrrhenian margin of the Campania  
39  
40 44 Plain graben have strongly influenced the growth and decline of many human settlements over the  
41  
42 45 millennia (Marzocchella 2000; Albore Livadie et al. 2001, 2003; Talamo and Ruggini 2005; Albore  
43  
44 46 Livadie 2007; Di Lorenzo et al. 2013). Evidence of the involvement of humans with volcanic  
45  
46 47 activity has been found in many areas close to the eruption vents, as well as in locations several tens  
47  
48 48 of kilometers further east and north-east. Interruptions in human occupation of these areas  
49  
50 49 alternated several times with resettlement phases, following the periods of activity and quiescence  
51  
52 50 of the local volcanism.  
53  
54  
55  
56 51 Numerous explosive and effusive eruptions have been produced by the volcanoes still active, but  
57  
58 52 the events of greatest intensity are associated with Somma-Vesuvius and the Campi Flegrei caldera.  
59  
60



1  
2  
3 53 In detail, the Plinian eruptions known as Pomici di Mercato ( $8890 \pm 90$   $^{14}\text{C}$  yr cal BP, Santacroce et  
4  
5 54 al. 2008), Pomici di Avellino ( $3945 \pm 10$   $^{14}\text{C}$  yr cal BP, Sevink et al. 2011) and Pompeii (AD 79,  
6  
7 55 Sigurdsson et al. 1985) were produced by Somma-Vesuvius, while the Agnano-Monte Spina  
8  
9 56 eruption ( $4625\text{-}4482 \pm 70$   $^{14}\text{C}$  yr cal BP, de Vita et al. 1999; Smith et al. 2011) had its origin in the  
10  
11 57 Campi Flegrei. Among them, the Avellino Pumice eruption (PdA) had a very strong impact on a  
12  
13 58 wide area, striking both the Campanian Plain and the surrounding Apennine Mountains. Before this  
14  
15 59 eruption, the Campania region was densely inhabited by Early Bronze Age (EBA) communities of  
16  
17 60 farmers and pastoralists (Albore Livadie 2007 and references therein), as testified by the discovery  
18  
19 61 of numerous villages and cultivated fields. In particular, the PdA eruption dramatically interrupted  
20  
21 62 and buried numerous remains of the notably well-developed socio-economic and demographic  
22  
23 63 scenario (Talamo 1993a; Talamo 1993b; Di Lorenzo et al. 2013) belonging to the archaeological  
24  
25 64 *facies* of Palma Campania. This *facies* is a cultural sphere developed in the EBA in the southern  
26  
27 65 Italy, starting from the Campania region and principally involving the inner Tyrrhenian lands, even   
28  
29 66 remains have also been found in Sicily, Aeolian Isles, Malta and northern Lazio region. The Palma   
30  
31 67 Campania *facies* is of exceptional relevance due to the specificity of the ceramic forms (Albore  
32  
33 68 Livadie, 1980) of Helladic derivation, therefore does not represent a simple evolution of the  
34  
35 69 previous Eneolithic culture. The *facies* ranks temporarily between the protoapenninico A and B (Lo  
36  
37 70 Porto, 1962) and is named after the place where in 1972 a new kind of pottery was found and  
38  
39 71 described (Albore Livadie et al. 1998).  
40  
41  
42  
43  
44  
45 72 In spite of the *Campania felix* is wellknown for the fertility of lands,  a real fertility evaluation based  
46  
47 73 on the main chemical and physical properties of the soils inhabited by the past communities in the  
48  
49 74 last 9000 years is not yet available in literature. The present study refers to the 1995 excavation  
50  
51 75 (Albore Livadie 1999), conducted in the vicinity of the 1972 excavation. In 1995, a dig in  
52  
53 76 Balle/Pirucchi locality at Palma Campania (Naples) brought to light i) a deep (approximately 9 m)  
54  
55 77 soil chronosequence (*sensu* Hugget 1998), composed of pyroclastic deposits and buried soils, which  
56  
57 78 started below the Pomici di Mercato (PdM) eruption (8890 yr cal BP) up to the present soil surface,  
58  
59  
60

1  
2  
3 79 along with ii) an extensive (approximately 4500 m<sup>2</sup>) well preserved paleo-surface of the EBA.  
4  
5 80 Archaeological remains from the soil chronosequence enabled the identification of soils of the Late  
6  
7 81 Imperial Roman, Late Republican Roman, Middle Bronze and Early Bronze Age, Eneolithic and  
8  
9 82 Mesolithic period. Moreover, the excavations have revealed traces left by human activity and  
10  
11 83 domestic animals above the EBA paleo-surface, along with a peculiar soil topography of uncertain  
12  
13 84 (natural or anthropic) genesis and use. Because of the exceptional degree of preservation and  
14  
15 85 importance of the archaeological excavation, a detailed stratigraphic (volcanological) and  
16  
17 86 pedological study was performed on both the entire soil chronosequence and the EBA paleosurface,  
18  
19 87 with the aim: i) of contributing to a better understanding of environmental conditions and land use  
20  
21 88 where these past human communities lived, by investigating the main chemical and  
22  
23 89 micromorphological properties of the soils of different age; ii) of identifying relationships between  
24  
25 90 particular soil properties (i.e. properties more sensitive to hydrological changes) and the estimated  
26  
27 91 pedogenetic times (EPT), by the use of volcanological evidence and climatic phases reported in the  
28  
29 92 literature, so as to enable the use of these properties as a proxy for the reconstruction of past  
30  
31 93 climatic conditions, in association with other paleoclimatic records; iii) to document the distribution  
32  
33 94 of the soil properties in three areas of the EBA paleosurface, previously subject to archaeological  
34  
35 95 investigation, in order to better understand the use of the entire area and the genesis (natural or  
36  
37 96 anthropic) of a debated micro-topography found in the South area.  
38  
39  
40  
41  
42  
43  
44

## 98 2. MATERIALS AND METHODS

### 99 2.1 Environmental and archaeological setting

100 The modern village of Palma Campania (southern Italy) is located on flat ground between the  
101 western slopes of the Sarno hills (Apennine Chain) and the eastern slopes of the Somma-Vesuvius  
102 volcano (whose crater is 11 km away). Due to its position close to Somma-Vesuvius an abundant  
103 accumulation of Vesuvian pyroclastic deposits affected the area, and Phlegrean products are also  
104 found (Orsi et al. 2004; Di Vito et al. 2013 and references therein).

1  
2  
3 105 In autumn 1995, approximately 2 km south-west of the modern village of Palma Campania, an  
4  
5 106 almost flat area of 4500 m<sup>2</sup> in Balle/Pirucchi location was investigated before the extension of an  
6  
7 107 existing land-fill site. The site is 200 m distant from the first discovered hut, where more than a  
8  
9 108 hundred vessels of the EBA Palma Campania *facies* were found in 1972, during the construction of  
10  
11 109 the Caserta - Salerno highway (Albore Livadie 1980). Moreover, in a further survey (1978) for a  
12  
13 110 highway lay-by construction at a distance of about 300 m, a burnt earth (“concolato”) floor was  
14  
15 111 sampled for the first <sup>14</sup>C analysis of the site (Albore Livadie 1980) and in 1987, wrought lens   
16  
17 112 hut floor with pottery fragments were found in a side of the land-fill cut (Pozzi 1987). The three  
18  
19 113 huts occupied a small hill (62 m asl) where the protohistoric village very likely stood, on the eastern  
20  
21 114 side of the present study area (Fig. 1a) that is at a slightly lower altitude (50.5 -52.9 m asl). On the  
22  
23 115 basis of the archaeological discoveries (Albore Livadie 1998), the EBA paleosurface was divided  
24  
25 116 into three main areas (North, Central and South) (Fig. 1b). In the North area two long narrow NE-  
26  
27 117 SW oriented trenches were found; they were 42 and 21 m long, both 35 cm wide, and 13 m apart.  
28  
29 118 The longer trench intersected a third one that was 3.5 m long, forming a sketch of quadrangle. This  
30  
31 119 arrangement suggested they were boundaries made by humans to demarcate plots of land allocated  
32  
33 120 to different family groups (Albore Livadie 1998). Inside and outside this area, numerous animal  
34  
35 121 hoof prints (238 tracks) were found, mainly belonging to adult cattle (*Bos taurus*) and also a few  
36  
37 122 young, but the number of livestock is indeterminable. These tracks (Fig. 2a) indicate that part of the  
38  
39 123 sector was used for pasturing animals and another part for animal transition, as shown by a  
40  
41 124 predominant NE-SW track orientation. In the Central area a few bone remains (teeth, long-bone and  
42  
43 125 skull fragments from adult cattle - *Bos taurus* - and an old pig *Sus scrofa*) were found, associated  
44  
45 126 with pottery fragments (large jars, cups and plates); these were interpreted as waste from the nearby  
46  
47 127 village. Moreover, a squared plot of land (12 x 13 m, 156 m<sup>2</sup>) with parallel NE - SW oriented  
48  
49 128 furrows 55 cm apart was also found (Fig. 2b). These furrows were interpreted as a “strip”   
50  
51 129 cultivation (Albore Livadie 1999) ploughed in one single direction using a simple scratch plough. A  
52  
53 130 riverbed 2 m wide, filled with redeposited volcanic pumice, separated the Central and South areas.  
54  
55  
56  
57  
58  
59  
60

1  
2  
3 131 The analyzed soil chronosequence (section-a) was sampled in the Central area, very close to the  
4  
5 132 riverbed. In the South area was found a slightly depressed zone (approximately 150 m<sup>2</sup>) with an  
6  
7 133 unusual micro-topography featuring ripples (micro-relief and micro-concavity), spaced at a distance  
8  
9 134 of approximately 40 cm one from another (Fig. 2c). The genesis (natural or anthropic) of this soil  
10  
11 135 micro-topography is still controversial. A soil trench (section-b) was dug in this area. Paired wheel  
12  
13 136 ruts were also found in the South area, oriented parallel to the riverbed pathway.

14  
15 137 Within the soil chronosequence, two areas rock dry wall built belonging to the Late Imperial  
16  
17 138 Roman age were found in correspondence to the *sola LROM2* and *LROM3*. They had first been  
18  
19 139 used as funerary enclosures in a Roman cemetery and successively for food storage and as stables.  
20  
21 140 Moreover, 14 tombs of the Late Republican Roman graveyard were found in soils with the  
22  
23 141 stratigraphic position of *MBLR1* and *MBLR2*, while ten tombs belonging to the Samnite burial  
24  
25 142 ground were found in *MBLR4* and *MBLR5*.

## 26 27 28 29 30 31 144 2.2 Materials

32  
33 145 Thirty bulk soil samples were collected from the chronosequence (section-a), located in the Central  
34  
35 146 area of the excavation and 8 from the EBA paleosurface. In detail, for the EBA paleosurface, 1  
36  
37 147 sample was sampled from the North area (s1), 1 from the Central area (s2) and 6 from the South  
38  
39 148 area where a trench (section-b) was dig till 1.5 m of depth. In this trench 2 soil profiles (P1 and P2)  
40  
41 149 were described and sampled, with P1 crossing both Mk and MC, and P2 approximately along a MR  
42  
43 150 (Fig. 4a). The soil sampling for the P1 was carried out only in the MC. In general, the soils of the  
44  
45 151 chronosequence were cultivated natural soils collected close to archaeological remains; they did not  
46  
47 152 show clear evidence of marked anthropic activity due to settlements (i.e. huts, tombs, rooms etc.).  
48  
49 153 On the basis of both volcanological deposits and archaeological remains (Albore Livadie 1998), 5  
50  
51 154 main groups of soils were identified within the chronosequence. The time-span in which each soil  
52  
53 155 developed has been defined as Estimated Pedogenetic Time (EP<sub>T</sub>) and calculated as the time which



1  
2  
3 156 elapsed between one eruption and another, using the age  $^{14}\text{C}$  BP of the identified pyroclastic records  
4  
5 157 (Table 1).

6  
7 158 By the use of the Kubiena boxes (5 x 10 x 3.5 cm) (Kubiena 1938) and the sampling of soil  
8  
9 159 aggregates, 37 undisturbed samples were collected from section-a and 9 from section-b for soil  
10  
11 160 micromorphology analyses.

12  
13  
14 161

### 15 162 2.3 Methods

16  
17 163 Bulk soil samples, dried at 40°C in an oven and sieved at 2 mm, were analyzed in accordance with  
18  
19 164 Soil Survey Staff (2009). The analysis of the particle size distribution (PSD) was performed with  
20  
21 165 the pipette method on samples dispersed with sodium hexametaphosphate (Na-HMP). This is the  
22  
23 166 dispersant agent recommended by the ISO international standards of soil particle size distribution  
24  
25 167 (PSD). Nevertheless, Na-HMP is known to fail in the complete dispersion of Andosols (Nanzyo et  
26  
27 168 al. 1993; Mizota and van Reeuwijk 1989). Therefore, considering such colloidal dispersion  
28  
29 169 problems, the sum of fine silt + clay was used as a parameter for discussing the soils' physical  
30  
31 170 properties (Terribile et al. 2000). The soil reaction was measured potentiometrically on soil-H<sub>2</sub>O  
32  
33 171 (1:2.5 ratio) suspensions, the cation exchange capacity (CEC) was measured with BaCl<sub>2</sub>-  
34  
35 172 triethanolamine (pH 8.2), following Mehlich (1938), and the exchangeable cations (Ca, Mg, Na, K)  
36  
37 173 content by ICP-AES. The organic matter (OM) content was determined following the Walkley and  
38  
39 174 Black (1934) procedure and the carbonates using the Dietrich-Fruehling calcimeter, after addition  
40  
41 175 of HCl 1M. The acid ammonium-oxalate extractable forms (Al<sub>o</sub>, Fe<sub>o</sub> and Si<sub>o</sub>), used to calculate the  
42  
43 176 Al<sub>o</sub>+ 0.5 Fe<sub>o</sub> index for the Andosol classification, were obtained as indicated by Schwertmann  
44  
45 177 (1964) and Blakemore et al. (1987). The total P content was determined by the ignition method: a  
46  
47 178 sulphuric acid extraction of soil samples ignited at a temperature of 550°C was performed. The  
48  
49 179 inorganic phosphorous (IOP) was measured after sulphuric acid extraction on non-ignited samples.  
50  
51 180 Both measurements of P content were carried out spectrophotometrically by the use of the ascorbic  
52  
53  
54  
55  
56  
57  
58  
59  
60

1  
2  
3 181 acid method. Then the organic phosphorous (OP) content was obtained by subtracting the inorganic  
4  
5 182 P content from the total P (Bethell and Matè 1989).

6  
7 183 All analyses were carried out on single soil horizons and then assembled in *sola* in order to better  
8  
9 184 evaluate different pedogenetic phases. A *solum* (plural *sola*) is the upper and the most weathered  
10  
11 185 part of the soil profile (i.e. A and B horizons) (*sensu* Soil Science Society of America 1987).

12  
13 186 A scheme of Land Evaluation (FAO 1976), aimed to produce a comparative evaluation of soil  
14  
15 187 fertility between *sola*, was set up. Such a scheme considered land qualities typical of the soil  
16  
17 188 fertility classification such as: soil thickness, CEC, base saturation, OM content and particle size  
18  
19 189 distribution (i.e. the clay + fine silt sum). The range for each land quality was divided into 4 classes  
20  
21 190 (first class for the least fertile and fourth for the most fertile). The sum of indexes obtained from  
22  
23 191 each class, assembled for each *solum*, enabled an empirical index of soil fertility (EIF) to be  
24  
25 192 constructed. In the present case study, the index ranged from 6 (the lowest fertility) to 16 (the  
26  
27 193 highest fertility).

28  
29 194 Soil thin sections (30  $\mu\text{m}$ ) were prepared from undisturbed soil samples and described according to  
30  
31 195 FitzPatrick (1993).

32  
33 196

### 34 35 36 37 197 **3. RESULTS AND DISCUSSION**

38  
39 198 Development and conservation of both soils and volcanic deposits in the archaeological site of  
40  
41 199 Palma Campania were the result of accretive processes strongly enhanced by the geomorphological  
42  
43 200 position in a gently sloping area where accumulation prevails over erosion. The following section  
44  
45 201 lists soil properties (morphological, chemical and physical), soil micro-morphology and discusses  
46  
47 202 environmental interpretation of i) the pedological/archaeological stratigraphic levels identified  
48  
49 203 within the soil chronosequence (section-a) (Table 2) and ii) the different areas of the EBA  
50  
51 204 paleosurface (i.e. North (s1) and Central areas (s2), along with section-b in the South area) (Table  
52  
53 205 3). As explained in the previous paragraph (2.1), the site investigated represented a territory outside  
54  
55  
56  
57  
58  
59  
60

206 the protohistoric village used for cultivation and animal pasturing activities, along with waste  
207 deposition.

208

209 3.1 Morphological, chemical and physical soil properties and soil micro-morphology

210 3.1.1 Mesolithic (*MES*) and Eneolithic (*ENEOL*) soils

211 *ENEOL* developed between PdM and Agnano-Monte Spina (AMS) eruptions, whereas *MES* was  
212 buried by PdM and was the oldest *solum* analysed from the chronosequence. *ENEOL* and *MES* were  
213 very different in terms of OM content (41.9 - 36.0 vs. 14.1-12.2 g kg<sup>-1</sup>, respectively) and thickness  
214 of the surface horizons (30 vs. 15 cm), whereas both soils were characterised by high CEC (36.5 -  
215 30.1 vs. 29.2- 34.7 cmol<sup>(+)</sup> kg<sup>-1</sup>) and moderate Al<sub>o</sub>+0.5Fe<sub>o</sub> index (1.2 – 1.0 %). These properties  
216 mean that these soils are highly fertile chemically and physically (EIF = 17 and 16 in *ENEOL* and  
217 *MES*, respectively). The moderate Al<sub>o</sub>+0.5 Fe<sub>o</sub> index (which is diagnostic for andic and vitric  
218 properties) is in agreement with the vitric properties, therefore these soils can be classified in the  
219 Andosols Reference Group (IUSS Working Group WRB 2014). The OP content resulted low to  
220 moderate in all the upper horizons (120 and 307 mg kg<sup>-1</sup>, in *ENEOL* and *MES* respectively) and  
221 decreased weakly with depth, while the calculated ratio P<sub>tot</sub>/P<sub>inorg</sub> (then called P ratio) was low  
222 for both *ENEOL* and *MES* (1.1 and 1.2-1.3) and compatible with low animal or anthropic  
223 frequentation in these soils. In such a framework, it must be considered that P ratios about 1.0 have  
224 been found in dwelling areas, with high phosphate inputs, and about 1.5 in locations of animal  
225 stabling and manured fields because of the association with a high organic matter content  
226 (Engelmark and Linderholm 1996; Macphail *et al.* 2000). In the Campania region a few settlements  
227 and cemeteries of Eneolithic age have been found in the area of Gricignano d'Aversa (Marzocchella  
228 2000), a village 30 km from Palma Campania.

229 The micromorphology of *ENEOL* showed clear signs of a high degree of weathering of the soil, such  
230 as fine granular structure, presence of weathered mineral fragments, brownish to reddish colour of  
231 the soil matrix (particularly in the Bwb horizons) and common (2-5%) iron segregations (Fig. 5i). In


1  
2  
3 232 *MES* the upper horizon exhibited a massive soil structure and frequent (5-10%) iron segregations, as  
4  
5 233 well as occurrence of weathered minerals and clay and silty-clay coatings (Fig. 5l). The presence of  
6  
7 234 this particular soil process, i.e. clay illuviation, is consistent with the specific climatic conditions  
8  
9 235 (see paragraph 3.2) and the moderate to high degree of soil weathering.  
10

11 236

### 14 237 3.1.2 Early Bronze Age (*EBAS*): the soil chronosequence and the paleosurface

16 238 *EBAS* developed in the period between Agnano-Monte Spina (AMS) and PdA eruptions and  
17  
18 239 corresponds to the soil where much protohistoric archaeological evidence was found.

20 240 Within the soil chronosequence (section-a) *EBAS* showed a thin (12 cm) A horizon characterised by  
21  
22 241 low OM (5.8 g kg<sup>-1</sup>), moderate CEC (16.9 cmol kg<sup>-1</sup>), low Al<sub>0</sub>+0.5Fe<sub>0</sub> index (0.2-0.4%) (below the  
23  
24 242 limit for vitric properties) and low OP and IOP fractions (226 and 652, respectively), which imply a  
25  
26 243 P ratio between 1.1 and 1.3. As a whole, the above data differed from measurements regarding the  
27  
28 244 pasture zone (s1) and ploughed fields (s2) of the central area, where the OM content was  
29  
30 245 significantly higher (13.5 and 9.8 g kg<sup>-1</sup> in s1 and s2, respectively) and the Al<sub>0</sub>+0.5Fe<sub>0</sub> index slightly  
31  
32 246 higher (0.5-0.6%)(within the vitric properties range).

34 247 Thin section analyses of the samples from the chronosequence revealed rare (0.5-2%) iron  
35  
36 248 segregations and coatings, along with frequent (10-15%) calcium carbonate segregation  (Fig. 5g  
37  
38 249 and 5h); both of these soil features are consistent with water circulation and processes of periodic  
39  
40 250 stagnation (hydromorphy) in the soil. Moreover, the presence of a sub-angular blocky structure and  
41  
42 251 planar pores identify a moderate degree of soil development where natural (e.g. fluvial) and/or  
43  
44 252 anthropic actions produced horizontal compaction. As reported in paragraph 2.1, archaeological  
45  
46 253 investigation showed the presence of an ancient stream on the *EBAS* paleo-surface, whose pathway  
47  
48 254 was very close to the analysed section-a (Fig. 1b). Therefore it is likely that during flooding events  
49  
50 255 this watercourse eroded part of the A horizon, determining a loss of OM. This hypothesis is in  
51  
52 256 agreement with the presence of CaCO<sub>3</sub> (1 g kg<sup>-1</sup>) in the soil, the low values of organic and inorganic  
53  
54 257 P fractions (indicating no anthropic or animal frequentation of the soil), and with its  
55  
56  
57  
58  
59  
60

1  
2  
3 258 micromorphological features. On the contrary, in the Central and North areas were found the  
4  
5 259 highest P ratios of the entire chronosequence (1.8 and 2.1 in s1 and s2, respectively), due to the  
6  
7 260 significantly high organic phosphorus content of these soils. As stated above, similar P ratio values  
8  
9 261 are reported in the literature for areas of animal stabling and manured fields (Engelmark and  
10  
11 262 Linderholm 1996; Macphail et al. 2000). Indeed, P is the only persistent element that is a sensitive  
12  
13 263 indicator of human presence, because the addition of P to the soil comes from human and animal  
14  
15 264 waste, from the presence of burials or cattle and soil fertilization with organic material (Holliday  
16  
17 265 and Gartner 2007). Therefore these results seem to confirm the land-use suggested by the  
18  
19 266 archaeological remains (see paragraph 2.1).

22 267 Much more difficulty was encountered interpreting the microtopography found in the South area  
23  
24 268 (Fig. 2c), made by **micro-reliefs** (MR) and micro-concavities (MC), approximately 20 to 60 cm  
25  
26 269 distant from each other. Observations showed that the MR had a shallow mineral horizon (Bwb<sub>1</sub>  
27  
28 270 *EBAS* section-b –P2 in Table 3), yellowish brown in colour (10YR5/4) at the top (Fig. 4b1). This  
29  
30 271 horizon was horizontally discontinuous and had an abrupt boundary with the underlying organ-  
31  
32 272 mineral horizon (Ab *EBAS* section-b – P2 in Table 3), which was dark brown (10YR 3/3) in colour.  
33  
34 273 This Ab covered another Bw horizon (named Bwb<sub>2</sub>), which was very similar in colour and  
35  
36 274 morphology to Bwb<sub>1</sub>. MC showed a different soil horizon sequence (Fig. 4b2), consisting of two  
37  
38 275 **organ-mineral** horizons at the top (Ab<sub>1</sub> and Ab<sub>2</sub> *EBAS* section-b – P1 in Table 3) and an underlying  
39  
40 276 Bwb. By the comparison of MC and MR chemical data, Ab of the former evidenced a higher OM  
41  
42 277 (22.5-22.9 in P1 and 17.5 g kg<sup>-1</sup> in P2, respectively), as well as a finer PSD (fine silt + clay = 356-  
43  
44 278 400 g kg<sup>-1</sup> and = 275-299 g kg<sup>-1</sup> in MC and MR, respectively), whereas both OM and PSD of Bwb  
45  
46 279 and Bwb<sub>2</sub> of MC and MR, respectively, were more similar (OM = 7.1 and 5.7 g kg<sup>-1</sup>, fine silt + clay  
47  
48 280 = 447 and 464 g kg<sup>-1</sup>). The CEC was particularly high in all Ab horizons (28.0-29.4 cmol kg<sup>-1</sup>), but  
49  
50 281 decreased in the **Bwbs** in the subsurface horizons of both MC and MR (i.e. Ab<sub>2</sub> and Ab  
51  
52 282 respectively) the P ratios were very high (2.1 and 1.7) and surprisingly similar to those found for the  
53  
54 283 pasture and ploughed fields (1.8 and 2.1 in s1 and s2, respectively). The soil micromorphology of  
55  
56  
57  
58  
59  
60

1  
2  
3 284 MR showed a combination of the following features: i) strongly heterogeneous matrix on the  
4  
5 285 surface; ii) complex crumb/granular microstructure in the upper few millimetres (Fig. 6a), followed  
6  
7 286 by a massive structure with frequent finer textured laminar aggregates, horizontally and vertically  
8  
9 287 oriented (Fig. 6b); iii) main planar pores (Fig. 6a) and rare secondary vesicle pores; (iv) presence of  
10  
11 288 organic residues mixed with charcoal (Fig. 6c) in the subsurface (Ab) and not in the surface (Bwb);  
12  
13 289 (v) weathered, fragmented and strained charcoal embedded in the massive soil structure (Fig. 6d).

14  
15  
16 290 In MC, compared with MR, (i) such heterogeneity of the soil matrix significantly decreased,  
17  
18 291 because the microstructure was complex (crumb and massive) in the first few millimetres (Fig. 6e),  
19  
20 292 but the porosity increased with depth (Fig. 6f); (ii) organic residues and charcoal also occurred on  
21  
22 293 the surface, but in smaller amounts; (iii) the soil PSD was visibly finer and (iv) abundant fauna  
23  
24 294 passages occurred at depth (Fig. 6f).

25  
26  
27 295 We therefore conclude that the vertical sequence of soil horizons found in MR is unusual, because  
28  
29 296 in a natural soil sequence the organ-mineral A horizon overlies the mineral Bw horizon, especially  
30  
31 297 in the local pedo-environmental conditions (rainfall, temperature, soil pH, clay minerals, etc.),  
32  
33 298 which do not promote any translocation of OM, as in the case of Spodosols (WRB 2014) in which  
34  
35 299 an inversion of the horizon position is possible. Hence, it is likely that in MR the original soil  
36  
37 300 structure was broken and reworked, producing heterogeneity and mixing of the soil fabric,  
38  
39 301 associated with soil compaction, as inferred from the presence of laminar aggregates, horizontal  
40  
41 302 planar pores and the vertical orientation of laminar aggregates in the massive structure. The OM  
42  
43 303 enrichment and high P ratio of the soil subsurface horizons of both MR and MC could be due to  
44  
45 304 OM input, probably from waste, animal excrement and manuring practices, as already found in s1  
46  
47 305 and s2. The abundance of charcoal fragments, more in the subsurface than on the surface, is another  
48  
49 306 anthropogenic feature indicating the practice of burning to prepare the underlying surface for a  
50  
51 307 specific use (such as in Courty et al. 1989). It is likely also that wet conditions occurred in MC, due  
52  
53 308 to the depressed morphology that also created a suitable environment for soil fauna, as indicated by  
54  
55 309 the higher frequency of fauna passages and channel structure. The higher  $Al_0+0.5Fe_0$  index of the  
56  
57  
58  
59  
60



1  
2  
3 310 top of the microtopography (in Ab<sub>1</sub> and Bwb of P1 and P2, respectively), compared with the other  
4  
5 311 parts of the paleo-surface, along with the presence of 'footprints' of *Phragmites*, a plant species  
6  
7 312 typical of hydromorphic environments, (Albore Livadie 1998) strongly supports the interpretation  
8  
9 313 of a wet environment, also favoured by the finer PSD of MC. Therefore, the probable explanation  
10  
11 314 for this morphology is that only human activity could produce such a combination of  
12  
13 315 morphological, chemical and micromorphological soil features. The area was first subjected to  
14  
15 316 clearance by burning and then strongly reworked, creating MC and MR, and manured. The wet  
16  
17 317 conditions of soils probably did not favour the use of the area for agriculture, so it was subsequently  
18  
19 318 abandoned and colonized by wild plants. The hypothesis of abandonment is consistent with both the  
20  
21 319 low P ratios of the upper horizons and the absence of traces such as ploughed furrows.  
22  
23  
24  
25  
26

27 321 *3.1.3 The soils after PdA and before Pompeii: from the Middle Bronze Age to the Late Republican*  
28  
29 322 *Roman era (MBLR)*

30  
31 323 The long period (approximately 1.5 kyr) that elapsed between two of the major Vesuvian eruptions  
32  
33 324 (PdA and Pompeii) was influenced by the occurrence of low-energy or subplinian events called AP  
34  
35 325 eruptions. For AP4 and AP5 there is not a certain chronology, while for AP6, AP3, AP2 and AP1  
36  
37 326 the dates (following Rolandi et al. 1998; Santacrose et al. 2008; Stothers and Rampino 1983) are  
38  
39 327 reported in Table 1.  
40  
41  
42

43 328 Within this group of *sola*, *MBLR1* and *MBLR2* showed the highest Al<sub>o</sub>+0.5Fe<sub>o</sub> index (1.2-1.8%) and  
44  
45 329 OM content (13.5-21.0 g kg<sup>-1</sup>), while *MBLR3* was intermediate (Al<sub>o</sub>+0.5Fe<sub>o</sub> = 0.7% and OM = 7.2 g  
46  
47 330 kg<sup>-1</sup>); a similar trend was found for the CEC (see Table 2). Except *MBLR6*, all *sola* met the vitric  
48  
49 331 properties and can be classified as Andosols. Data of Al<sub>o</sub>+0.5Fe<sub>o</sub> index and OM content are strongly  
50  
51 332 consistent with those found by Vogel and Märker (2011) in the Roman paleosols of Boscoreale. The  
52  
53 333 soil fertility varied from high (EIF = 14-13) in *MBLR2* and *MBLR1* to low (EIF = 6 -7) in *MBLR4*,  
54  
55 334 *MBLR5* and *MBLR6*, while intermediate (EIF = 10) was in *MBLR3*. Moreover, *MBLR1* and *MBLR2*  
56  
57 335 had the highest P ratio of the sequence (1.3 and 1.6), as a consequence of high and very high OP  
58  
59  
60

1  
2  
3 336 contents (272-369 mg kg<sup>-1</sup> and 543-727 mg kg<sup>-1</sup> in *MBLR1* and *MBLR2* respectively), which is a  
4  
5 337 strong indicator of human and/or animal frequentation of the soils. Therefore soil fertility and P data  
6  
7 338 are in accordance with the archaeological remains that indicate an intensively inhabited landscape  
8  
9 339 during the Roman epoch, a cemetery dating to which was also found associated with cultivated  
10  
11 340 soils.

12  
13 341 The micromorphological analyses showed a very fine granular microstructure and occurrence of  
14  
15 342 thick weathering rims in both *MBLR1* and *MBLR2*, confirming the moderate to high degree of  
16  
17 343 pedogenetic development indicated by the chemical properties. Moreover, the presence of rare fine  
18  
19 344 laminar structures in *MBLR1* and the very dark brown matrix of *MBLR2* (see Table 2) could be  
20  
21 345 considered signs of a higher degree of weathering in *MBLR2* than in *MBLR1*. A similar micro-  
22  
23 346 structure, but nearly massive (i.e. primary volcanic ash structure), was found for *MBLR4*, in which  
24  
25 347 rare laminar aggregates were also found. *MBLR5* and *MBLR6* were mainly massive, with strongly  
26  
27 348 weathered areas containing iron segregations, very likely as a consequence of temporary  
28  
29 349 waterlogging in this dense layer with low porosity.

30  
31 350 As a whole, chemical and micromorphological properties of the *sola* before AP5 (*MBLR3*, *MBLR4*,  
32  
33 351 *MBLR5*, *MBLR6*) evidenced a significantly lower degree of weathering than the *sola* after AP5  
34  
35 352 (*MBLR1* and *MBLR2*).

36  
37  
38  
39  
40  
41 353

#### 42 43 354 *3.1.4 The soils after Pompeii: Late Roman (LROM) till Early Modern (EMOD) period*

44  
45 355 The *EMOD* and the *LROM sola* (*LROM1*, 2 and 3) formed in the time period between the AD 79  
46  
47 356 (i.e. Pompeii) (Santacroce et al. 2008) and AD 1631 eruptions. In detail, *EMOD* developed between  
48  
49 357 AD 512 (Wulf et al. 2004) and AD 1631, *LROM1* between AD 472 (i.e. Pollena, Sulpizio et al.  
50  
51 358 2005) and AD 512, *LROM2* between AD 472 and AD 203 (Cioni et al. 2008), *LROM3* between AD  
52  
53 359 203 and AD 79 eruptions. Differently from the other eruptive events, ash lenses from AD 203 were  
54  
55 360 not found in this excavation, but they were reported by Di Vito et al. (2013) in a nearby excavation  
56  
57 361 (location: Via Isernia, approximately 3 km away). Among the above mentioned eruptions, the sub-  
58  
59  
60



1  
2  
3 362 Plinian event of AD 472 produced the most widespread effects and sealed evidence of human  
4  
5 363 activity (Di Vito et al. 2013).  
6  
7 364 *EMOD* showed elevated OM content (16.8-18.6 g kg<sup>-1</sup>) and CEC (28.1-26.1 cmol kg<sup>-1</sup>), whereas the  
8  
9 365 Al<sub>o</sub>+0.5 Fe<sub>o</sub> index (1.8-2.7 %) was very high (the highest of the chronosequence) and met the andic  
10  
11 366 properties requirements. On the contrary *LROM1* was very low in both OM (3.3 g kg<sup>-1</sup>) and Al<sub>o</sub>+0.5  
12  
13 367 Fe<sub>o</sub> index (0.4%), the latter at the boundary of vitric-non vitric properties, whereas it showed  
14  
15 368 moderate CEC (15.9 cmol<sup>+</sup> kg<sup>-1</sup>). Both *EMOD* and *LROM1* had high total P content (P<sub>tot</sub> = 1652-  
16  
17 369 1940 and 2185 mg kg<sup>-1</sup>, respectively), mainly due to the inorganic fraction (P<sub>inorg</sub> = 1609-1759  
18  
19 370 and 2178 mg kg<sup>-1</sup>, respectively). A renewed increase in OM (5.6-13.4 g kg<sup>-1</sup>) and Al<sub>o</sub>+0.5 Fe<sub>o</sub> index  
20  
21 371 (1.3-1.5 %) was found in the underlying *LROM2* and 3, where the CEC was moderate to high (13.4-  
22  
23 372 22.3 cmol<sup>+</sup> kg<sup>-1</sup>), whereas the total P content (1360-1388 mg kg<sup>-1</sup>) decreased. However, the P ratio  
24  
25 373 was always low (around 1.0), indicating a low anthropic or animal frequentation in these soils, as  
26  
27 374 well as in the more recent *LMOD solum*. In this group of *sola*, only *EMOD* showed a high fertility  
28  
29 375 value (EIF = 13), whereas the lowest value was found for *LROM2* (EIF = 8).  
30  
31  
32  
33  
34 376 In a comparison between *EMOD* and the overlying *LMOD*, the micromorphological analyses  
35  
36 377 showed a relative loss of porosity and increase of mineral weathering in *EMOD*, as well as  
37  
38 378 occurrence of frequent laminar pedofeatures and charcoal fragments (Fig. 5b and 5c). These pedo-  
39  
40 379 features are related to anthropic activities, such as compaction, when associated with organic matter  
41  
42 380 increase (Courty et al. 1989) and charcoal presence. A different microscopic arrangement was  
43  
44 381 shown by *LROM1*, with higher porosity on the top and massive structure at the bottom, occurrence  
45  
46 382 of rounded soil aggregates, iron segregations in the soil matrix and silty coatings around pumice and  
47  
48 383 mineral fragments (Figs. 5d and 5e, respectively), with iron segregations inside probably due to  
49  
50 384 weathering, reworking and erosion processes that occurred during explosive eruptions. These  
51  
52 385 properties are very likely related to intense and frequent meteoric precipitation and alluvial events  
53  
54 386 which occurred during and after the AD 472 eruption and are well documented in the  
55  
56 387 volcanological literature (Sulpizio et al. 2006). These events created an unstable environment  
57  
58  
59  
60

1  
2  
3 388 unfavourable to both pedogenetic processes and human activities, as demonstrated by the low  
4  
5 389  $Al_0+0.5 Fe_0$  index and OM content. In both *LROM2* and 3 the micromorphological analyses showed  
6  
7 390 i) granular structure, ii) presence of poorly weathered fragments of minerals and scoria and iii) silty  
8  
9 391 textural features (Fig. 5f)(i.e. ashy laminar structures) related to the deposition of volcanic materials  
10  
11 392 on the soil surface. As a whole, these characteristics indicate a moderate degree of soil  
12  
13 393 development.  
14

15  
16 394

### 17 18 395 *3.1.5 The soils after the AD 1631 eruption: the Late Modern Age (LMOD)*

19  
20 396 *LMOD1* and 2 developed in the time from the AD 1631 eruption (dated by Rolandi et al. 1993; Rosi  
21  
22 397 et al. 1993) to the present; therefore, even if not clearly identified in field, pyroclastic materials  
23  
24 398 from Vesuvius' recent activity following the 1631 eruption must have affected the genesis of this  
25  
26 399 *solum*.

27  
28  
29 400 The *LMOD1* and 2 showed moderate to low OM content ( $15.2-6.2\text{-g kg}^{-1}$ ) with respect to the entire  
30  
31 401 soil sequence (Table 2), which is consistent with the cation exchange capacity ( $CEC = 24.3-2.1$   
32  
33 402  $\text{cmol kg}^{-1}$ ). The  $Al_0+0.5 Fe_0$  index was moderate to weakly developed (from 1.5 to 0.9 %), but in  
34  
35 403 accordance with the vitric properties and can be classified in the Andosols Reference Group. The  
36  
37 404 total P (from 2150 to 1873  $\text{mg kg}^{-1}$ ) was generally high, likely as a consequence of the high IOP  
38  
39 405 ( $1852 - 1986 \text{ mg kg}^{-1}$ ), while the P ratio was low. Therefore *LMOD1* and 2 were classified as being  
40  
41 406 of high and low fertility ( $EIF = 12$  and 7), respectively. The micromorphological analyses showed  
42  
43 407 frequent occurrence of weakly weathered mineral crystals, pumices and scoria, associated with  
44  
45 408 single grains and granular structure (Fig. 5a) with abundant pore space, which confirmed the  
46  
47 409 moderate to low degree of soil weathering indicated by the chemical analyses.  
48  
49

50  
51 410

### 52 53 411 *3.2 Soil properties and climatic factors: possible relationships*

54  
55 412 In the literature, the use of multiproxy records (e.g.  $\delta^{18}O$ , pollen,  $\delta^{13}C$ , stable isotopes, etc.) has  
56  
57 413 allowed a picture of climatic variability to be defined, in terms of temperature and rainfall, for the  
58  
59  
60

1  
2  
3 414 Holocene period in many areas of Europe and Italy (Magny et al. 2009; Zanchetta et al. 2012;  
4  
5 415 Regattieri et al. 2014). On the other hand, a knowledge gap exists regarding the relationship  
6  
7 416 between climatic phases and soil properties, which could constitute key parameters when a territory  
8  
9 417 is investigated in terms of human history. Indeed, soil properties are directly related to the fertility  
10  
11 418 of the land and thus to the density of human occupation. The climate is one of the most important  
12  
13 419 soil forming factors (Jenny 1947; Tardy 1986), since it determines rates of processes by controlling  
14  
15 420 moisture availability and temperature, the identification of particular soil properties more sensitive  
16  
17 421 to these two parameters and easy to measure in soils would be of great interest in archaeological  
18  
19 422 contexts.

20  
21  
22  
23 423 An attempt is therefore made here to evaluate the relationship between documented climatic  
24  
25 424 changes and selected soil properties measured along the chronosequence, assuming that the  
26  
27 425 geomorphological conditions of the site have not changed very much with the time, because the  
28  
29 426 spatial distribution of soil properties could change with geomorphological position, as demonstrated  
30  
31 427 for roman paleosols in neighbours areas (Vogel and Märker 2011). The time of pedogenesis has  
32  
33 428 also been taken into account in this evaluation. The soil properties used for this purpose are the soil  
34  
35 429 OM content and the  $Al_0+0.5Fe_0$  index, due to their high reactivity to climatic changes. Indeed, the  
36  
37 430 amount of OM and humic substances in the soil depends on both the quantity and quality of  
38  
39 431 residues and organic fertilizers which reach the soil, as well as the rapidity of mineralization and  
40  
41 432 humification processes to which the residues are subject. The OM mineralization (i.e. the  
42  
43 433 conversion of nutrients from organic to inorganic forms) is influenced by several factors such as  
44  
45 434 temperature, availability of oxygen and humidity, pH, etc. On the other hand, temperature and  
46  
47 435 precipitation also have a controlling influence on the formation of Andosols, according with the  
48  
49 436 andic properties (Shoji et al. 1993), because higher temperature increases the rate of chemical  
50  
51 437 weathering in tephras and higher precipitation intensifies the leaching of Si and bases, leading to the  
52  
53 438 formation of allophanes instead of Si-rich clay minerals. In the case of the  $Al_0+0.5Fe_0$  index, since  
54  
55 439 the  $Al_0$ ,  $Fe_0$  and  $Si_0$  represent the active, short-range-order (i.e. allophane, imogolite, ferrihydrate)

1  
2  
3 440 or amorphous (Al-humus complexes and opaline silica) Al, Fe and Si compounds in soils  
4  
5 441 (Blakemore et al. 1987), this percentage is used here as a measure of all these forms.

6  
7 442 The ages of tephras used for the EPT calculation of the *sola* are given in table 3, while the OM  
8  
9 443 content, the  $Al_0+0.5Fe_0$  index and the EPT vs. the *sola* of the chronosequence are reported in figures  
10  
11 444 7a and 7b. *MES*, which is characterized by generally low  $Al_0+0.5Fe_0$  index and OM, was formed in  
12  
13 445 the period preceding PdM (8.9 kyr cal BP), when phases of climatic improvement after the Last  
14  
15 446 Glacial period alternated with cold episodes (e.g. the Younger Dryas), which interrupted the  
16  
17 447 deglaciation before the beginning of the Holocene. We observe that the effects of these alternating  
18  
19 448 climatic conditions were the moderately low development of soil properties and the activation of  
20  
21 449 clay illuviation processes, as showed by the micromorphological analysis. As reported in the  
22  
23 450 literature, this process typically occurs in soils when i) distinct dry periods are followed by high  
24  
25 451 intensity rainfall and ii) fine clays (generally phyllosilicates) are present and move through non-  
26  
27 452 capillary voids suspended in the percolating water. In general, phyllosilicates are scarce in  
28  
29 453 Andosols, but periodic desiccation of allophanes may cause recrystallization to phyllosilicates  
30  
31 454 (Buurman and Jongmans 1987; Jongmans et al. 1994). Due to the absence of the older  
32  
33 455 chronological constraint, the EPT was not calculated to evaluate the influence of this factor on soil  
34  
35 456 properties. Nevertheless, the soil properties suggest the presence of a stable geomorphological  
36  
37 457 environment suitable for anthropic frequentation, without any catastrophic eruptive events.

38  
39 458 The highest values of the  $Al_0+0.5Fe_0$  index + % OM of the chronosequence, associated with the  
40  
41 459 highest EPT (see Figures 7a and b), are found for *ENEO*, which formed between PdM and AMS  
42  
43 460 eruptions (8.9 - 4.5 kyr cal BP) in a period falling almost entirely in the Neolithic Climatic  
44  
45 461 Optimum or Hypsithermal period (ca. 8.2-5.5 kyr cal BP) of the early Holocene. The largely stable  
46  
47 462 warm and humid climatic conditions favored the greatest expansion of the oak forests in the eastern  
48  
49 463 Mediterranean region (Cheddadi et al. 1991), in Greece (Bottema 1974) and on the southern  
50  
51 464 Dalmatian islands (Beug 1975). Therefore the very high OM content (3.9%) found for *ENEO* is  
52  
53 465 very likely due to plant residues, owing to the forest cover, which were incorporated into the soil  
54  
55  
56  
57  
58  
59  
60

1  
2  
3 466 and poorly mineralized because of the humid climate. The  $Al_0+0.5Fe_0$  index was expected to be  
4  
5 467 very high due to the very stable environment, but was found to be only moderate probably as a  
6  
7 468 consequence of i) recrystallization of allophanes as phyllosilicates or ii) inhibition of allophane  
8  
9 469 formation caused by perhumid, highly leaching climate, which removed all silica from the soil.  
10  
11 470 The overlying *EBAS*, which developed between the AMS and PdA eruptions (4.5 to 3.9 kyr cal BP),  
12  
13 471 showed a low  $Al_0+0.5Fe_0$  index and low OM content, the latter being markedly lower than *ENEO*.  
14  
15 472 The very low developed properties do not seem to result from a short EPT, because approximately  
16  
17 473 600 yr could have been a sufficiently long period to produce moderate soil properties in favorable  
18  
19 474 (i.e., warm and moist) climatic conditions. The decrease of both  $Al_0+0.5Fe_0$  and OM seems  
20  
21 475 therefore to be related to two essential environmental changes that occurred before the PdA event: i)  
22  
23 476 climatic: Jalut et al. (2000) identify an aridification phase at ca. 5300-4200 yr cal BP, Magny et al.  
24  
25 477 (2009) report a pronounced lowstand in lakes responsible for peat formation before PdA deposition,  
26  
27 478 as well as Zanchetta et al. (2012) who identify a prominent arid event at ca. 4100 – 4000 yr cal BP,  
28  
29 479 which is in agreement with other multi-proxy records (Drysdale et al. 2006) or the Spanish flood  
30  
31 480 history records (Thorndycraft and Benito 2006) and ii) vegetational (land use): the Campania region  
32  
33 481 was intensely occupied by the Proto-Apenne civilization and agriculture flourished during the  
34  
35 482 Bronze Age.  
36  
37 483 With regard to the subsequent period, we observed that: i) from *MBLR6* to *MBLR4* (formed after  
38  
39 484 PdA till AP4) the  $Al_0+0.5Fe_0$  index and the OM are very low and their EPT varies from 173 to 534  
40  
41 485 yr (on average 220 yr), ii) from *MBLR2* to *LROM2* (after AP5 till AD 472) the  $Al_0+0.5Fe_0$  index  
42  
43 486 and the OM are higher, always moderate (except for the OM in *LROM2*), with an EPT varying from  
44  
45 487 124 to 269 yr (on average 217 yr), iii) *MBLR3* has intermediate properties (between AP4 and AP5).  
46  
47 488 Due to the absence of a certain chronology for AP4 and AP5, the EPT of *MBLR4*, *MBLR3* and  
48  
49 489 *MBLR2* was assumed to be approximately 180 yr. Thus the soil before AP5 also formed in a similar  
50  
51 490 or longer EPT compared with the more recent soils, which showed less developed properties. In the  
52  
53 491 period after PdA until AP4-AP5 (i.e. *sola* from *MBLR6* to *MBLR4*), the studied area was affected  
54  
55  
56  
57  
58  
59  
60

1  
2  
3 492 by frequent eruptions with ash emission and deposition (Di Vito et al. 2013) that played an  
4  
5 493 important role in the low degree of soil weathering because they i) frequently interrupted the  
6  
7 494 pedogenetic processes, decreasing the soil formation rate, ii) likely modified the local climate,  
8  
9 495 increasing the water input into the atmosphere and meteoric precipitation which caused marked ash  
10  
11 496 reworking after eruptive events. Moreover, two further significant phases of drier climatic  
12  
13 497 conditions occurred at ca. 3500 and 3300 yr cal BP (Zanchetta et al. 2012), which correspond to the  
14  
15 498 phase of cooling following the deposition of the Thera tephra (Rohling et al. 2002). A severe  
16  
17 499 drought was found also by Bretschneider and Van Lerbege (2008) between ca. 3300 and 2700 yr cal  
18  
19 500 BP, indicated by pollen evidence in alluvial deposits. With regard to this arid phase, Kaniewski et  
20  
21 501 al. (2010) have suggested that this event may have produced region-wide crop failure corresponding  
22  
23 502 to the Late Bronze Age collapse. However, after AP4 (starting from *MBLR3*) the soil properties  
24  
25 503 show a gradual increase, except for a small decrease in correspondence to *LROM2*. No certain  
26  
27 504 climatic references were found for the period from *MBLR3* to *MBLR1*, while evidence of wetter  
28  
29 505 conditions during the Roman Empire (1800-1500 yr cal BP), which clearly favored the pedogenesis  
30  
31 506 of *LROM3* and *LROM2*, were reported by Zanchetta et al (2012). At that time, the plains around  
32  
33 507 Vesuvius were densely populated and intensely cultivated by Roman or Romanized populations.  
34  
35 508 However, the increase of  $Al_0+0.5 Fe_0$  index (from 0.4 to 2.7 %) and OM content (from 3.3 to 18.6 g  
36  
37 509  $kg^{-1}$ ) is surprisingly consistent with the EPT, which grew from *LROM1* to *LROM2*, *LROM3* (EPT =  
38  
39 510 40, 269 and 124 yr, respectively) and *EMOD* (EPT approximately 1100 yr), strongly supporting  
40  
41 511 these soil properties as indicators of stability for these ancient paleo-surfaces. For the last two *sola*  
42  
43 512 *EMOD* and *LROM2*, it is interesting to observe that the  $Al_0+0.5Fe_0$  index and the OM is higher for  
44  
45 513 the first solum than the latter, consistently with the EPT (approximately 1100 and 380 yr,  
46  
47 514 respectively). In this regard, two relevant phases of wetter conditions occurred at ca. 1350-1250 yr  
48  
49 515 cal BP (600-700 AD, at the beginning of the Early Medieval period) and 1100-800 yr cal BP (850-  
50  
51 516 1150 AD, during the subsequent Middle Ages) (Bradley et al. 2003) which could have improved the  
52  
53 517 soil properties of *EMOD*, but one only wetter phase centered at ca. 90 cal BP (AD 1860) in the  
54  
55  
56  
57  
58  
59  
60



1  
2  
3 518 period of *LMOD*. Moreover, the time range of *EMOD* included the Medieval Warm Period (MWP)  
4  
5 519 (Mann et al. 2009), a medieval climate optimum generally thought to have occurred from about AD  
6  
7 520 950 to 1250, during the European Middle Ages, while in *LMOD* the Little Ice Age (LIA) occurred,  
8  
9 521 lasting approximately from AD 1300 to 1850 (Grove 2004; Matthews and Briffa 2005). In spite of  
10  
11 522 the good relationship found between soil properties and EPT and climatic conditions, we prefer to  
12  
13 523 be cautious in the case of *LMOD* because of its proximity to the surface, where recent ploughing  
14  
15 524 practices and/or deposition of recent Vesuvius products might also have affected the soil formation.  
16  
17  
18  
19

525

#### 526 4. CONCLUSIONS

527 The present case study at Palma Campania shows one of the better-preserved chronosequences of  
528 the Campania region, in a peri-volcanic environment. Vesuvius and Phlegrean products represent  
529 both the parent material from which the soils developed and the material that has covered, buried  
530 and preserved the pre-existing soils and evidence of human activity. As a whole, the results indicate  
531 that the choice by human communities to live in this particular area is due to the moderate to high  
532 potential fertility of its soils, which show different degrees of pedogenesis, according to the  
533 different weathering environments, geomorphological stability and time (duration) of soil processes.  
534 Regarding to ~~the~~ EBA paleo-surface, the soil properties demonstrated a good correlation with the  
535 land use documented by archaeological evidence in the North and the Central area. For the South  
536 area, we conclude that only human activity could produce such a combination of soil morphological  
537 (i.e. micro-relief and micro-concavities, disordered vertical sequence of soil horizons), chemical  
538 (i.e. high OM and organic P contents) and micromorphological (i.e. laminar aggregates, horizontal  
539 planar pores and vertical orientation of laminar aggregates) features. Indeed, we suppose that the  
540 area had been previously subject to clearance by burning and then strongly reworked and manured.  
541 The hypothesis of abandonment after this human intervention is supported by absence of specific  
542 shapes (like ploughing traces, etc.) probably due to hydromorphic conditions. A more  
543 interdisciplinary dataset (pollen, phytoliths, etc.) would help to better define the use of the area.

1  
2  
3 544 Against this background, the relationship found between both the OM content and some andic  
4  
5 545 properties (i.e. the  $Al_0+0.5Fe_0$  index), and the EPT and climatic conditions reported in the literature,  
6  
7 546 is of great interest. We are confident that these properties, in association with other paleoclimate  
8  
9 547 data, may be used as a proxy to better identify the Holocene climatic changes (i.e. cold and/or dry  
10  
11 548 phases) that occurred in volcanic environments.  
12  
13  
14 549

## 15 16 550 **5. REFERENCES**

17  
18 551 Albore Livadie, C. (1980). Palma Campania. Resti di abitato dell'età del Bronzo Antico. *Not. Sc.*  
19  
20 552 *XXXIV.*, 59-101.

21  
22 553 Albore Livadie, C. (1999). Territorio e insediamenti nell'agro Nolano durante il Bronzo antico  
23  
24 554 (facies di Palma Campania): Nota preliminare. In C. Albore Livadie (Ed), L'eruzione  
25  
26 555 vesuviana delle "Pomici di Avellino" e la facies di Palma Campania. *Atti del Convegno*  
27  
28 556 *Internazionale, Centro Universitario Europeo per i Beni Culturali Ravello, Ravello 15-17*  
29  
30 557 *luglio 1994, Bari 1999, 203-243.*

31  
32 558 Albore Livadie, C. (2007). L'età del Bronzo antico e medio nella Campania nord-occidentale, in  
33  
34 559 *Atti della XL Riunione Scientifica I.I.P.P. Firenze, 179-203.*

35  
36 560 Albore Livadie, C., Mastrolorenzo, G., Vecchio, G. (1998). Eruzioni pliniane del Somma-Vesuvio e  
37  
38 561 siti archeologici dell'area nolana, in *Archeologia e vulcanologia*. In P. G. Guzzo & R. Peroni  
39  
40 562 (Eds) Campania, Napoli, 39-73.

41  
42 563 Albore Livadie, C., Castaldo, N. , Mastrolorenzo, G. , Vecchio, G. (2001). Effetti delle eruzioni del  
43  
44 564 Somma-Vesuvio sul territorio di Nola dall'età del Bronzo all'epoca romana tardiva, in *Tephros*  
45  
46 565 – *chronologie et archéologie*, Congresso internazionale "Téphrochronologie et co-existence  
47  
48 566 *hommes-volcans*", Brives-Charensac 24-29 agosto 1998, *Dossiers de l'Archéo-Logis*, 1,119-  
49  
50 567 118.  
51  
52  
53  
54  
55  
56  
57  
58  
59  
60



- 1  
2  
3 568 Albore Livadie, C., Cazzella, A., Marzocchella, A., Pacciarelli, M. (2003). La struttura degli abitati  
4  
5 569 del Bronzo antico e medio nelle Eolie e nell'Italia meridionale, in *Atti della XXXV Riunione*  
6  
7 570 *Scientifica I.I.P.P.* Firenze, vol. I, 113-142.
- 8  
9 571 Bethell, P. and Máté, I. (1989). The use of soil phosphate analysis in archaeology: a critique. In J.  
10  
11 572 Henderson (Ed.), *Scientific Analysis in Archaeology*, Oxford University Press, 1-29.
- 12  
13 573 Beug, H-J. (1975). Changes of climate and vegetation belts in the mountains of Mediterranean  
14  
15 574 Europe during the Holocene. *Bulletin of Geology* 19, 101-110.
- 16  
17 575 Blakemore, L.C., Searle, P.L., Daly, B.K. (1987). Methods for Chemical Analysis of Soils. N.Z.  
18  
19 576 *Soil Bureau Sci. Rep.* 80. Soil Bureau, Lower Hutt. New Zealand.
- 20  
21 577 Bottema, S. (1974). Implication of a pollen diagram from the Adriatic Sea. *Geologie en Mijnbouw*  
22  
23 578 53, 401-405.
- 24  
25 579 Bradley, R.S., Hughes, M.K., Diaz, H.F. (2003). Climate in medieval Time. *Science* 302, 404-405.
- 26  
27 580 Bretschneider, J. and Van Lerbege, K. (2008). Tell Tweini, ancient Gibala, between 2600 BCE and  
28  
29 581 333 BCE. In In search of Gibala, an archaeological and historical study based on eight  
30  
31 582 seasons of excavations at Tell Tweini (1999-2007) in A and C fields, In Bretschneider J, Van  
32  
33 583 Lerbege K 2008. (Eds.) *Aula Orientalis*: Barcelona, 12-66.
- 34  
35 584 Buurman, P. and Jongmans, A.G. (1987). Amorphous clay coatings in a lowland Oxisol and other  
36  
37 585 andesitic soils of West Java, Indonesia. *Pemberitaan Penelitian Tanah dan Pupuk* 7:31-40.
- 38  
39 586 Cheddadi, R., Yu, G., Guiot, J., Harrison, S.P., Prentice, I.C. (1997). The climate of Europe 6000  
40  
41 587 years ago. *Climate Dynam.* 13, 1-9.
- 42  
43 588 Cioni, R., Bertagnini, A., Santacroce, R., Andronico, D. (2008). Explosive activity and eruption  
44  
45 589 scenarios at Somma-Vesuvius (Italy): Towards a new classification scheme. *Journal of*  
46  
47 590 *Volcanology and Geothermal Research* 178 (3), 331-346
- 48  
49 591 Courty, M.A., Goldberg, P., Macphail, R. (1989). Soils and micromorphology in archaeology.  
50  
51 592 Cambridge: Cambridge University Press.
- 52  
53  
54  
55  
56  
57  
58  
59  
60

- 1  
2  
3 593 de Vita, S., Orsi, G., Civetta, L., Carandente, A., D'Antonio, M., Di Cesare, T., Di Vito, M., Fisher,  
4  
5 594 R.V., Isaia, R., Marotta, E., Ort, M., Pappalardo, L. Piochi, M., Southon, J. (1999). The  
6  
7 595 Agnano-Monte Spina eruption (4,100 years BP) in the restless Campi Flegrei caldera (Italy).  
8  
9 596 *J. Volcan. Geotherm. Res.* 91, 269-301
- 10  
11 597 Di Lorenzo H., , Di Vito, M.A., Talamo, P., Bishop, J., Castaldo, N., de Vita, S., Nave, R., Marco  
12  
13 598 Pacciarelli (2013). The impact of the Pomici di Avellino Plinian eruption of Vesuvius on  
14  
15 599 early and middle Bronze age human settlement in Campania (Southern Italy). *Tagungen des L*  
16  
17 600 *andesmuseums für Vorgeschichte hall*, 9.
- 18  
19  
20 601 Di Vito, M.A., Castaldo, N., de Vita, S., Bishop, J., Vecchio, G. (2013). Human colonization and  
21  
22 602 volcanic activity in the eastern Campania Plain (Italy) between the Eneolithic and Late  
23  
24 603 Roman periods. *Quatern. Intern.* 303, 132-141.
- 25  
26  
27 604 Drysdale, R., Zanchetta, G., Hellstrom, J., Maas, R., Fallick, A., Pickett, M., Cartwright, I., Piccini,  
28  
29 605 L. (2006). Late Holocene drought responsible for the collapse of Old World civilizations is  
30  
31 606 recorded in an Italian cave flowstone. *Geology* 34, 101–104.
- 32  
33  
34 607 Engelmark, R. and Linderholm, J. (1996). Prehistoric land management and cultivation: a soil  
35  
36 608 chemical study. 6<sup>th</sup> Nordic conference on the application of Scientific Methods in  
37  
38 609 Archaeology, Esjberg 1993 (P.A.C.T.).
- 39  
40  
41 610 FAO (1976). A framework for Land Evaluation. Rome.
- 42  
43 611 FitzPatrick, E.A. (1993). Soil microscopy and Micromorphology. Wiley, Chichester, UK.
- 44  
45 612 Grove, J.M. (2004). Little Ice Ages: Ancient and Modern. Routledge, London (2 volumes).
- 46  
47 613 Holliday, T. and Gartner, W. (2007). Methods of soil P analysis in archaeology. *J Archaeol. Sci.* 34,  
48  
49 614 301-333.
- 50  
51  
52 615 ~~Huggett, R. J. (1998). Soil chronosequences, soil development, and soil evolution: a critical review.~~  
53  
54 616 ~~Catena 32, 155–172.~~

- 1  
2  
3 617 IUSS Working Group WRB (2014). World Reference Base for Soil Resources 2014, International  
4  
5 618 soil classification system for naming soils and creating legends for soil map, World Soil  
6  
7 619 Resources Reports No. 106, FAO, Rome  
8  
9  
10 620 Jalut, G., Esteban Amat, A., Bonnet, L., Gauquelin, T., Fontugne, M. (2000). Holocene climatic  
11  
12 621 changes in the Western Mediterranean, from south-east France to south-east Spain.  
13  
14 622 *Palaeogeography, Palaeoclimatology, Palaeoecology* 160, 255-290.  
15  
16 623 Jenny, H. (1941). Factors of Soil Formation: A System of Quantitative Pedology. McGraw-Hill,  
17  
18 624 New York, 281 pp.  
19  
20  
21 625 Jongmans, A.G., Van Oort, F., Buurman, P., Jaunet, A.M. (1994). Micromorphology and  
22  
23 626 submicroscopy of isotropic and anisotropic Al/Si coatings in a Quaternary Allier terrace. In:  
24  
25 627 A. Ringrose and G.D. Humphries (eds.). Soil Micromorphology: studies in management and  
26  
27 628 genesis. *Developments in Soil Science* 22: 285-291. Elsevier, Amsterdam.  
28  
29  
30 629 Kaniewski, D., Van Campo, E., Weiss, H. (2012). Drought is a recurring challenge in the Middle  
31  
32 630 East. *Proceedings of the National Academy of Sciences* 109: 3862–3867.  
33  
34 631 Kubiena, W.L. (1938). Micropedology, Collegiate Press, Ames, Iowa.  
35  
36 632 Lo Porto, G.F. (1962). La tomba di Cellino San Marco e l'inizio della civiltà del Bronzo in Puglia,  
37  
38 633 *Bull. Palet. It.*, 71-72, Firenze, 191-225  
39  
40  
41 634 Macphail R., Cruise G., Engelmark R., Linderholm J. (2000). Integrating soil Micromorphology  
42  
43 635 and rapid chemical Survey Methods: new developments in reconstructing past rural settlement  
44  
45 636 and landscape organisation. *Interpreting stratigraphy conferences, 1993-1997*  
46  
47 637 Magny, M., Vannièrè, B., Zanchetta, G., Fouache, E., Touchais, G., Petrika, L., Coussot, C.,  
48  
49 638 Walter-Simonnet, A., Arnaud, F. (2009). *The Holocene* 19 (6), 823-833.  
50  
51  
52 639 Mann, M. E., Zhang, Z., Rutherford, S., et al. (2009). Global Signatures and Dynamical Origins of  
53  
54 640 the Little Ice Age and Medieval Climate Anomaly. *Science* 326 (5957), 1256–60.  
55  
56 641 Marzocchella, A., 2000. Storie di contadini alle falde del Vesuvio. *Archeo* 182, 36–45.  
57  
58  
59  
60

- 1  
2  
3 642 Matthews, J.A. and Briffa, K.R. (2005). The 'Little Ice Age': re-evaluation of an evolving concept.  
4  
5 643 *Geogr. Ann.*, 87, A (1), pp. 17–36. Retrieved 17 July 2015.  
6  
7 644 Mehlich, A. (1938). Use of triethanolamine acetate-barium hydroxide buffer for the determination  
8  
9 645 of some base exchange properties and lime requirement of soil, *Soil Sci. Soc. Am. Pro.*, 29,  
10  
11 646 374–378.  
12  
13 647 Mizota, C. and Van Reeuwijk, L.P. (1989). Clay mineralogy and chemistry of soils formed in  
14  
15 648 volcanic material in diverse climatic regions. Soil Monograph 2, ISRIC, Wageningen, p. 185.  
16  
17 649 Nanzyo, M., Shoji, S., Dahlgren, R. (1993). Physical characteristics of volcanic ash soils. In:  
18  
19 650 Volcanic Ash Soils: Genesis, Properties and Utilization (S. Shoji, M. Nanzyo and R.  
20  
21 651 Dahlgren, Eds.), *Development in Soil Science*, vol. 17, Elsevier, Amsterdam, 189-201.  
22  
23 652 Orsi, G., Di Vito, M.A., Isaia, R. (2004). Volcanic hazard assessment at the restless Campi Flegrei  
24  
25 653 caldera. *Bulletin of Volcanology* 66, 514-530.  
26  
27 654 Regattieri, E., Zanchetta, G., Drysdale, R.N., Isola, I., Hellstrom, J.C., Dallai, L. (2014). *J. Quatern.*  
28  
29 655 *Sci.* 29 (4), 381-392.  
30  
31 656 Rohling, E.J., Mayewski, P.A., Abu-Zied, R.H., Caford, J.S.L., Hayes, A. (2002). Holocene  
32  
33 657 atmosphere–ocean interactions: records from Greenland and the Aegean Sea. *Climate*  
34  
35 658 *Dynamics* 18, 587–93.  
36  
37 659 Rolandi, G., Barella, A.M., Borrelli, A. (1993). The 1631 eruption of Vesuvius. *J. Volcanol.*  
38  
39 660 *Geotherm. Res.* 58, 183-201.  
40  
41 661 Rolandi, G., Petrosino, P., Mc Geehin, J. (1998). The interplinian activity at Somma-Vesuvius in  
42  
43 662 the last 3500 years. *J. Volcanol. Geotherm. Res.* 82, 19-52.  
44  
45 663 Rosi, M., Principe, C., Vecci, R. (1993). The 1631 eruption of Vesuvius reconstructed from the  
46  
47 664 review of chronicles and study of deposits. *J. Volcanol. Geotherm. Res.* 58, 151-182.  
48  
49 665 Santacroce, R., Cioni, R., Marianelli, P., Sbrana, A., Sulpizio, R., Zanchetta, G., Donahue, D. J.,  
50  
51 666 Joron, J. J. (2008). Age and whole rock-glass compositions of proximal pyroclastics from the  
52  
53  
54  
55  
56  
57  
58  
59  
60

- 1  
2  
3 667 major explosive eruptions of Somma-Vesuvius: a review as a tool for distal  
4  
5 668 tephrostratigraphy. *J. Volcanol. Geotherm. Res.* 177, 1–18.  
6  
7  
8 669 Schwertmann, U. (1964). Differenzierung der Eisenoxide des Bodens durch photochemische  
9  
10 670 Extraktion mit saurer Ammoniumoxalat-lösung. *Zeitschrift Pflanzenernahrung Düngung*  
11  
12 671 *Bodenkunde*, 105, 194-202.  
13  
14 672 Sevink, J., van Bergen, M. J., van der Plicht, J., Feiken, H., Anastasia, C., Huizinga, A., Maroto, J.,  
15  
16 673 Vaquero, M., Arrizabalaga, Á., Baena, J., Baquedano, E., Jordá, J., Julià, R., Montes, R.,  
17  
18 674 Rasines, P., Wood, R., Walsma, A. (2011). Robust date for the Bronze Age Avellino eruption  
19  
20 675 (Somma-Vesuvius): 3945 +/- 10 cal BP (1995 +/- 10 cal BC). In: *Quaternary Science*  
21  
22 676 *Reviews* 30 (9-10), 1035-1046.  
23  
24  
25  
26 677 Shoji, S., Dahlgren, R., Nanzyo, M. (1993). Genesis of volcanic ash soils, in: *Volcanic Ash Soils.*  
27  
28 678 *Genesis, Properties and Utilization. Developments in Soil Science*, 21, 37–71, Elsevier,  
29  
30 679 Amsterdam, London, New York, Tokyo.  
31  
32  
33 680 Sigurdsson H., Carey S., Cornell W., Pescatore T. (1985). The eruption of Vesuvius in AD 79: *Natl.*  
34  
35 681 *Geogr. Res.*, 1, 332-387.  
36  
37  
38 682 Smith, V. C., Isaia, R., Pearce, N. J. G. (2011). Tephrostratigraphy and glass compositions of post  
39  
40 683 15 kyr Campi Flegrei eruptions: implications for eruption history and chronostratigraphic  
41  
42 684 markers. *Quaternary Scien. Rev.* 30, 3638–3660. doi:10.1016/j.quascirev.2011.07.012.  
43  
44 685 [http://journals.ohiolink.edu/ejc/article.cgi?issn=o2773791&issue=](http://journals.ohiolink.edu/ejc/article.cgi?issn=o2773791&issue=v30i2526&article=3638_tagcopfehacm)  
45  
46 686 [v30i2526&article=3638\\_tagcopfehacm](http://journals.ohiolink.edu/ejc/article.cgi?issn=o2773791&issue=v30i2526&article=3638_tagcopfehacm) (28.11.2012).  
47  
48  
49 687 Soil Science Society of America (1987). *Glossary of Soil Science Terms*, Madison, Wisconsin  
50  
51 688 USA, p. 27.  
52  
53  
54 689 Soil Survey Staff (2009). *Soil Survey Field And Laboratory Methods Manual*. Soil Survey  
55  
56 690 Investigations Report No. 51 Version 1.0. National Soil Survey Center. Natural Resources  
57  
58 691 Conservation Service U.S. Department of Agriculture. Lincoln, Nebraska.  
59  
60

- 1  
2  
3 692 Stothers, R.B. and Rampino, M.,R. (1983). Volcanic eruptions in the Mediterranean before A.D.  
4  
5 693 630 from written and archaeological sources. *J. Geophys. Res.* 88, B8, 6357-6371.  
6  
7 694 Sulpizio, R., Mele, D., Dellino, P., La Volpe, L. (2005). A complex, Subplinian-type eruption from  
8  
9 695 low-viscosity, phonolitic to tephra-phonolitic magma: the AD 472 (Pollena) eruption of  
10  
11 696 Somma-Vesuvius, Italy. *Bulletin of Volcanology* 67, 743-767.  
12  
13 697 Sulpizio, R., Zanchetta, G., Demi, F., Di Vito, M.A., Pareschi, M.T., Santacroce, R. (2006). The  
14  
15 698 Holocene syneruptive volcanoclastic debris flows in the Vesuvian rea: geological data as a  
16  
17 699 guide for hazard assessment. In: Siebe, C., Mcias, J.L., Aguirre-Diaz, G.J. (Eds.), Neogene-  
18  
19 700 Quaternary Continental Margin Volcanism: a Perspective from México. *Geological Society of*  
20  
21 701 *America* Special Paper 402, Penrose Conference Series, 217-235.  
22  
23 702 Talamo, P. (1993 a). La facies di Palma Campania nell'ambito del Bronzo Antico italiano:  
24  
25 703 definizione culturale e rapporti interculturali. Tesi di Dottorato Univ. Napoli. Facoltà di  
26  
27 704 Lettere e Filosofia (Napoli 1993).  
28  
29 705 Talamo, P. (1993b). Capua (Caserta). Località Strepparo e Cento Moggie. Scavi nell'area degli  
30  
31 706 insediamenti preistorici CIRA 4. *Boll. Arch.* del Ministero Beni Culturali e Ambientali 22,  
32  
33 707 1993, 63–69.  
34  
35 708 Talamo, P. and Ruggini, C. (2005). Il territorio campano al confine con la Puglia nell'età del  
36  
37 709 Bronzo. In: A. Gravina (ed.), Atti 25° Convegno sulla Preistoria-Protostoria-Storia della  
38  
39 710 Daunia (San Severo 2005) 171–188.  
40  
41 711 Tardy, Y. (1986). Le cycle de l'eau. Climats, paleoclimats et géochimie globale. Masson, Paris,  
42  
43 712 169-209.  
44  
45 713 Terribile, F., Basile, A., De Mascellis, R., Di Gennaro, A., Mele, G., Vingiani, S. (2000). I suoli  
46  
47 714 delle aree di crisi di Sarno e Quindici: proprietà e comportamenti in relazione ai fenomeni  
48  
49 715 franosi del 1998. *Quaderni di Geologia Applicata*, 7(1), 59-79.  
50  
51 716 Thorndycraft, V.R. and Benito, G. (2006). Late Holocene fluvial chronology of Spain: the role of  
52  
53 717 climatic variability and human impact. *Catena* 66, 34–41.  
54  
55  
56  
57  
58  
59  
60

- 1  
2  
3 718 Vogel, S. and Märker, M. (2011). Characterization of the pre-AD 79 Roman paleosol south of  
4  
5 719 Pompeii (Italy): Correlation between soil parameter values and paleo-topography. *Geoderma*  
6  
7 720 160, 548–558.
- 9  
10 721 Zanchetta, G., Giraudi, C., Sulpizio, R., Magny, M., Drysdale, R.N., Sadori, L. (2012).  
11  
12 722 Constraining the onset of the Holocene “Neoglacial” over the central Italy using tephra layers.  
13  
14 723 *Quaternary Research* 78, 236-247.
- 16 724 Walkley, A. and Black, I.A. (1934). An examination of the Degtjareff method for determining  
17  
18 725 organic carbon in soils: Effect of variations in digestion conditions and of inorganic soil  
19  
20 726 constituents. *Soil Sci.* 63, 251-263.
- 23 727 Wulf, S., Kraml, M., Brauer, A., Keller, J., Negendank, J.F.W. (2004). Tephrochronology of the  
24  
25 728 100 ka lacustrine sediment record of Lago Grande di Monticchio (southern Italy). *Quat. Int.* 122,  
26  
27 729 7-30.  
28  
29 730  
30  
31  
32  
33  
34  
35  
36  
37  
38  
39  
40  
41  
42  
43  
44  
45  
46  
47  
48  
49  
50  
51  
52  
53  
54  
55  
56  
57  
58  
59  
60



## 731 CAPTIONS

732 Table 1. Estimated pedogenetic time (EPT) of the sola from the chronosequence by the  
733 volcanological records (eruptions).

734 Table 2 Main morphological, chemical and physical soil properties of the chronosequence (section-  
735 a).

736 Table 3. Main morphological, chemical and physical soil properties of the EBA paleo-surface  
737 (section-b, s1 and s2 samples).

738 Figure 1. a) Location of the study site showing previous nearby archaeological discoveries; b) the  
739 three main areas of the EBA paleo-surface and the location of section-a and section-b.

740 Figure 2. a) Scattered animal tracks in the North area; b) traces of cultivation activity in the Central  
741 area; c) microtopography of the South area.

742 Figure 3. a) Sketch of the section-a: chronosequence of volcanic deposits and soils

743 Figure 4. a) Position of section-b with respect to the micro-topography of the southern sector; b)  
744 profile 1 crosses microreliefs (MR) and concavities (MC), profile 2 is along a microrelief.

745 Figure 5. Micrographs of *sola* from the chronosequence, in plane polarised light (PPL) and crossed  
746 polarised light (XPL) of a) granular structure of *LMOD1*; b) compacted laminar features in *EMOD*  
747 (PPL); c) charcoal fragment in *EMOD* (PPL); d) iron segregations in the soil matrix of *LROM1*  
748 (PPL); e) silty coatings around a pumice fragment, with internal iron segregations, in *LROM1*  
749 (PPL); f) silty textural features in *LROM3* (PPL); g and h) pore network filled by calcium carbonate  
750 segregations in PPL and XPL; i) weathered soil matrix in *ENE0* (PPL); l) iron segregations and  
751 clay coatings in *MES* (PPL).

752 Figure 6. Micrographs of the Early Bronze Age microtopography in PPL. Microreliefs: a)  
753 crumb/granular structure in the upper few millimeters, where 2 red arrows indicate planar pores b)  
754 progressively massive structure with depth, with finer textured horizontally-oriented laminar  
755 aggregates (indicated by the red arrow); c) organic residues mixed with charcoal in the soil matrix;



1  
2  
3 756 d) fragment of strained charcoal embedded in the soil matrix; Microconcreteness: e) massive and  
4  
5 757 crumb structure on the surface, f) abundant fauna passages at depth.

6  
7 758 Figure 7. For each *solum* of the chronosequence are reported in a)  $Al_0+0.5Fe_0$  index (red) and the  
8  
9 759 OM (pink), both in %; b) estimated pedogenetic times (EPT) (blue) in years. The *solum* age  
10  
11 760 increases from the bottom upwards.

12  
13  
14 761  
15  
16  
17  
18  
19  
20  
21  
22  
23  
24  
25  
26  
27  
28  
29  
30  
31  
32  
33  
34  
35  
36  
37  
38  
39  
40  
41  
42  
43  
44  
45  
46  
47  
48  
49  
50  
51  
52  
53  
54  
55  
56  
57  
58  
59  
60

For Peer Review

<sup>14</sup> C yr BP	<sup>14</sup> C cal yr BP	Eruption	<i>Solum</i>	EPT
1747	1478		<b>LMOD</b>	384
470±55	520±40	<b>AD 1631</b>		
			<b>EMOD</b>	1119
1420	1420 varve age	<b>AD 512</b>		
			<b>LROM 1</b>	40
1530±70	1630±50	<b>AD 472</b>		
			<b>LROM 2</b>	269
1747	1747	<b>AD 203</b>		
			<b>LROM 3</b>	124
1871	1871	<b>AD 79</b>		
			<b>MBLR 1</b>	296
2167-2166 (217-216 BC)		<b>AP6</b>		
			<b>MBLR 2</b>	180
2347		<b>AP5</b>		
			<b>MBLR 3</b>	180
2527		<b>AP4</b>		
			<b>MBLR 4</b>	180
2710±60	2830±50	<b>AP3</b>		
			<b>MBLR 5</b>	534
3150±100 AP2 3500±60 AP1	3364 AP2 and 3818-3726 AP1	<b>AP1-AP2</b>		
			<b>MBLR 6</b>	173
3565±20	3945±10; 4310 varve yr BP	<b>PdA</b>		
			<b>EBAS</b>	608
4130±50	4625-4482±70	<b>AMS</b>		
			<b>ENEO</b>	4336
8098±71	8890±90	<b>PdM</b>		
			<b>MES</b>	

EPT = estimated pedogenetic time

Group of soils	Solum	Horizon	Depth (cm)	Colour (moist)	pH H <sub>2</sub> O	OM g kg <sup>-1</sup>	CEC cmol(+) kg <sup>-1</sup>	OP	IOP mg kg <sup>-1</sup>	Total P	P ratio	Al <sub>0</sub> + 0.5 Fe <sub>0</sub> %	Fine silt+clay g kg <sup>-1</sup>	CaC O <sub>3</sub>	Particle size classes <sup>a</sup>	EIF
EMOD-LMOD	LMOD1	A1	0-20	10YR3/1	7.2	15.2	24.3	164	1986	2150	1.1	1.5	125	0	loamy sand	12
	LMOD2	A2-A3	20-70	2.5Y3/2	7.2	9.9-6.2	2.1-6.8	154-40	1719-1852	1873-1892	1.1-1.0	1.4-0.9	93-99	0	loamy sand	7
	EMOD	3Ab1-3Ab2	85-130	10YR2/2	6.9	18.6	28.1	181-90	1759-1735	1940-1825	1.1	1.8-2.2	118-125	0	loamy sand	13
3Bwb		130-145	10YR3/2	7.5	16.8	26.1	43	1609	1652	1.0	2.7	140	0	loamy sand		
LROM	LROM 1	5Bwb	225-265	10YR3/2	7.4	3.3	15.9	7	2178	2185	1.0	0.4	338	0	sandy loam	10
	LROM 2	6Bwb	320-335	2.5Y4/2	7.0	5.6	13.4	150	1210	1360	1.1	1.3	125	0	loamy sand	8
	LROM 3	7AB	335-345	2.5Y4/2	7.0	13.4	22.3	164	1224	1388	1.1	1.5	175	0	loamy sand	12
MBLR	MBLR 1	8Bwb1-8Bwb2	355-400	2.5Y4/2	7.4-7.1	15.2	24.3	272-369	1027-948	1299-1317	1.3-1.4	1.4-1.8	240-251	0	sandy loam	13
	MBLR 2	9Ab1-9Ab2	400-460	2.5Y3/2	6.9-7.0	13.5-21.0	19.0-26.4	727-543	1131-1216	1858-1759	1.6-1.4	1.8-1.2	205-259	0	sandy loam	14
	MBLR 3	9Bwb	460-485	2.5Y4/2	7.2	7.2	12.6	210	1135	1345	1.2	0.7	186	0	sandy loam	10
	MBLR 4	10Bwb	510-525	2.5Y4/2	6.8	1.4	7.8	126	1381	1507	1.1	0.5	187	0	sandy loam	6
	MBLR 5	10CBb	540-585	5Y 4/1	7.1	0.5	2.6	n.d.	n.d.	n.d.	n.d.	0.5	158	0	n.d.	7
	MBLR 6	11Bwb	610-620	2.5Y4/2	7.1	2.6	6.8	287	1359	1646	1.2	0.2	210	0	sandy loam	6
EBAS	EBAS	13Ab	680-692	10YR3/3	7.6	5.8	16.9	226	652	878	1.3	0.4	421	0	sandy loam	11
		13Bwb	692-705	2.5Y5/3	7.6	1.9	13.5	110	837	947	1.1	0.2	292	0	sandy loam	
Eneo-MES	ENE0	14Ab1	710-720	10YR2/2	7.6	41.9	54.5	120	1340	1220	1.1	1.2	431	1	silt loam	15
		14Ab2	720-740	10YR3/2	7.5	36.0	47.8	122	1220	1342	1.1	1.2	450	0	silt loam	
	MES	14Bwb	740-755	10YR4/6	7.6	6.6	14.6	100	1002	1102	1.1	0.5	315	0	sandy loam	
		15Ab	760-775	2.5Y3/2	7.6	14.1	29.2	307	1207	1514	1.3	1.0	385	0	sandy loam	15
		15ABb	775-785	2.5Y4/3	6.9	12.2	34.7	307	1253	1560	1.2	0.9	305	0	sandy loam	
MES	15Bwb1/Bwb2	785-840	2.5Y5/4	7.1-6.9	7.1-4.8	28.1-23.8	245-276	1140-1196	1385-1472	1.2	0.5-0.4	254-297	0	sandy loam		
	15Bwb3-Bwb4	840-875	2.5Y5/5 - 2.5Y6/3	7.5-7.3	1.2-0.5	18.6-13.9	260-120	1168-1286	1428-1406	1.2-1.1	0.3	296-238	0	sandy loam		

OM = organic matter; CEC = cation exchange capacity; OP = organic phosphorous fraction; IOP = inorganic phosphorous fraction; Total P = OP + IOP; P ratio = Total P / IOP; Al<sub>0</sub> + 0.5 Fe<sub>0</sub> = ammonium oxalate Al and Fe extractable form; EIF = empirical index of fertility

Solum	Horizon	Depth (cm)	Colour (moist)	pH H <sub>2</sub> O	OM g kg <sup>-1</sup>	CEC cmol(+) kg <sup>-1</sup>	OP	IOP mg kg <sup>-1</sup>	Total P	P ratio	Al <sub>o</sub> + 0.5 Fe <sub>o</sub> %	Fine silt+clay g kg <sup>-1</sup>	CaCO <sub>3</sub>	Particle size classes	EIF
<b>P1</b>	Ab1	680-705	10YR4/2	7.7	22.5	28.0	179	462	641	1.4	1.1	356	0	sandy loam	14
	Ab2	705-725	10YR4/2	7.5	22.9	29.1	501	457	958	2.1	0.7	400	1	loam	
	Bwb	725-745	10YR5/4	7.6	7.1	19.0	154	482	636	1.3	1.2	447	1	loam	
<b>P2</b>	Bwb	680-687	10YR5/4	7.3	5.8	23.2	157	540	697	1.3	1.2	275	0	sandy loam	16
	Ab	687-712	10YR3/3	6.9	17.5	29.4	388	524	912	1.7	0.6	299	0	sandy loam	
	Bwb2	712-732	10YR5/4	6.9	5.7	17.8	53	570	623	1.1	1.4	464	0	sandy loam	
<b>s1</b>	Ab	680-690	10YR4/2	8	13.5	22.4	528	680	1208	1.8	0.6	322	0	sandy loam	14
<b>s2</b>	Ab	680-690	10YR4/2	7	9.8	18.2	525	475	1000	2.1	0.5	334	0	sandy loam	11

OM = organic matter; CEC = cation exchange capacity; OP = organic phosphorous fraction; IOP = inorganic phosphorous fraction; Total P = OP + IOP; P ratio = Total P / IOP;  
 Al<sub>o</sub> + 0.5 Fe<sub>o</sub> = ammonium oxalate Al and Fe extractable form; EIF = empirical index of fertility

1  
2  
3  
4  
5  
6  
7  
8  
9  
10  
11  
12  
13  
14  
15  
16  
17  
18  
19  
20  
21  
22  
23  
24  
25  
26  
27  
28  
29  
30  
31  
32  
33  
34  
35  
36  
37  
38  
39  
40  
41  
42  
43  
44  
45  
46  
47  
48  
49  
50  
51  
52  
53  
54  
55  
56  
57  
58  
59  
60

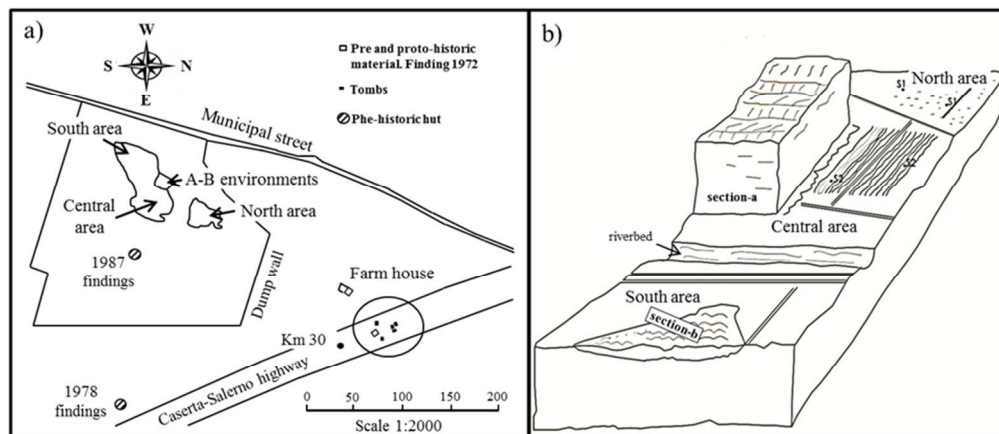


Figure 1. a) Location of the study site in the context of previous archaeological findings; b) the three main areas of the EBA paeosurface and the location of section-a and section-b.  
161x72mm (150 x 150 DPI)

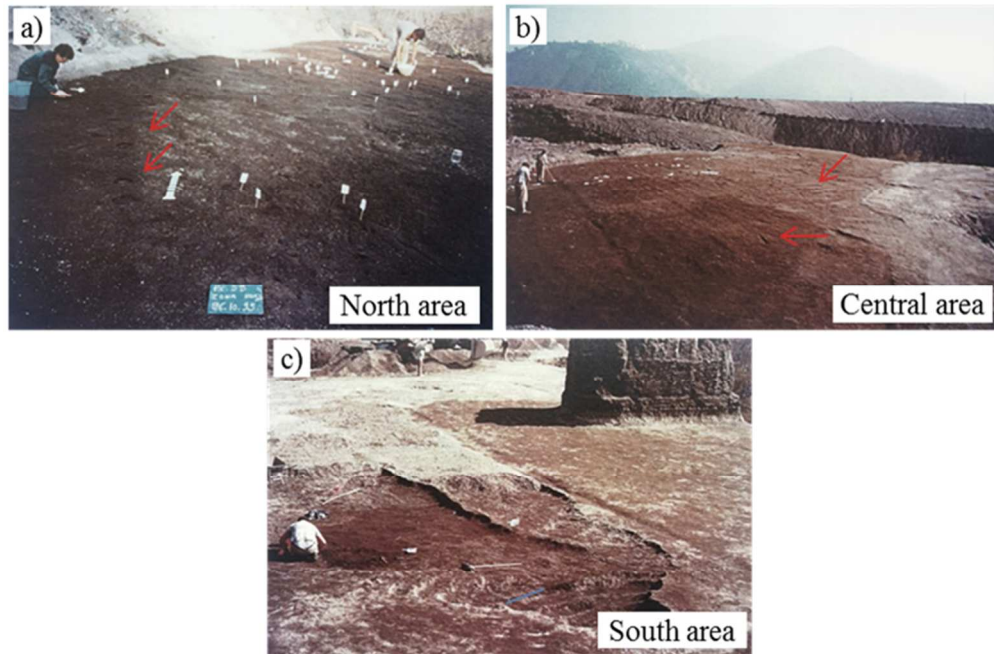


Figure 2. a) Chaotically scattered animal tracks in the North area; b) traces of agricultural activities in the Central area; c) microtopography of the South area.  
 160x107mm (150 x 150 DPI)

Review

1  
2  
3  
4  
5  
6  
7  
8  
9  
10  
11  
12  
13  
14  
15  
16  
17  
18  
19  
20  
21  
22  
23  
24  
25  
26  
27  
28  
29  
30  
31  
32  
33  
34  
35  
36  
37  
38  
39  
40  
41  
42  
43  
44  
45  
46  
47  
48  
49  
50  
51  
52  
53  
54  
55  
56  
57  
58  
59  
60

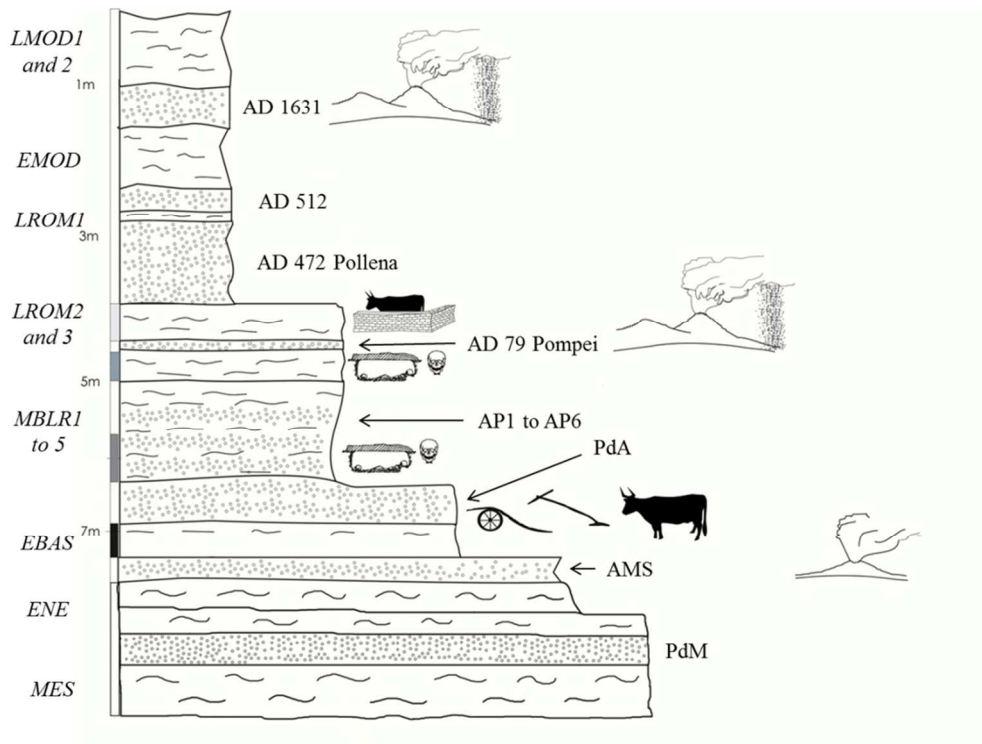


Figure 3. Sketch of the section-a: chronosequence of volcanic records and soils  
222x166mm (150 x 150 DPI)

1  
2  
3  
4  
5  
6  
7  
8  
9  
10  
11  
12  
13  
14  
15  
16  
17  
18  
19  
20  
21  
22  
23  
24  
25  
26  
27  
28  
29  
30  
31  
32  
33  
34  
35  
36  
37  
38  
39  
40  
41  
42  
43  
44  
45  
46  
47  
48  
49  
50  
51  
52  
53  
54  
55  
56  
57  
58  
59  
60

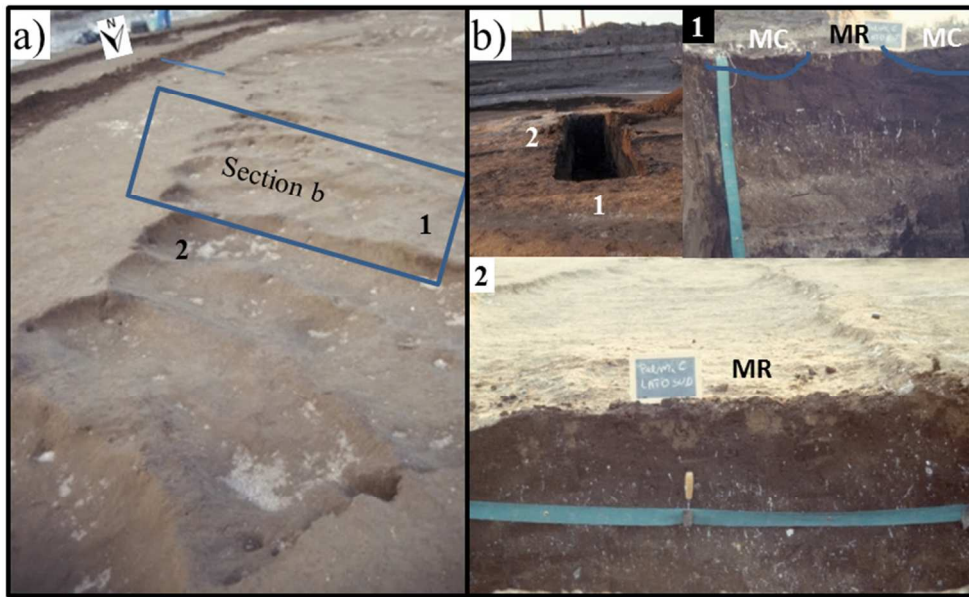


Figure 4. a) Position of the section-b with respect to the micro-topography of the southern sector; b) the profile 1 crosses microreliefs (MR) and concavities (MC), the profile 2 is along a microrelief.  
149x90mm (150 x 150 DPI)



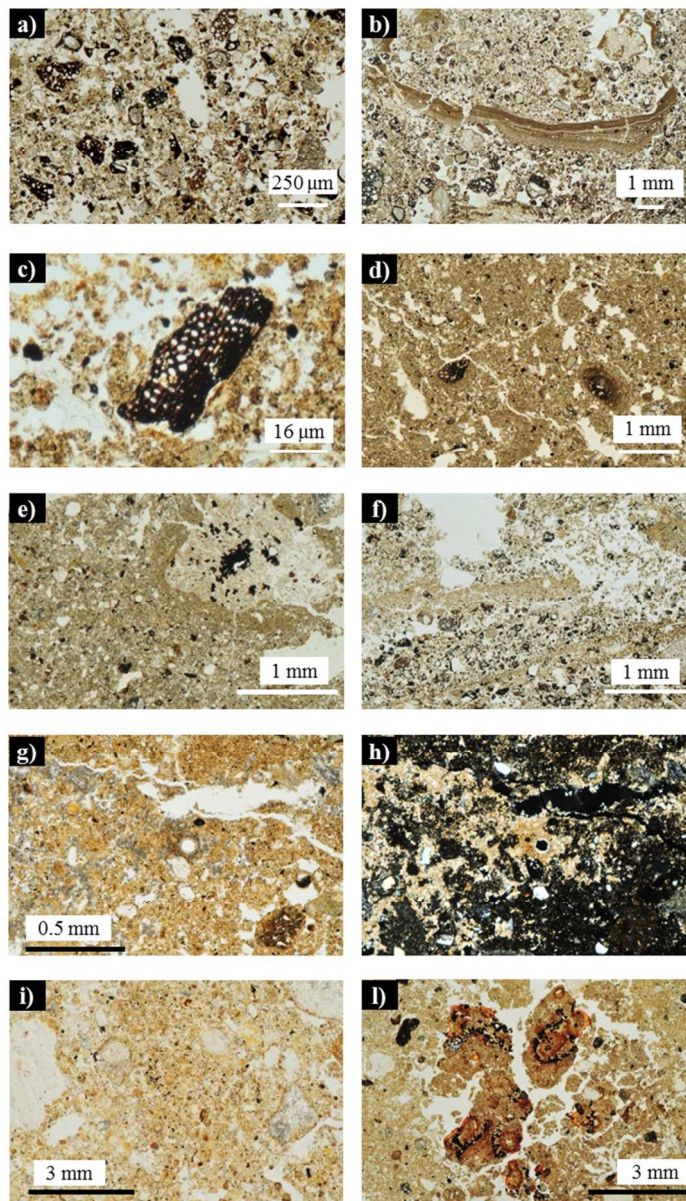


Figure 5. Micrographs of sola from the chronosequence, in plane polarised light (PPL) and crossed polarised light (XPL) of a) granular structure of LMOD1; b) compacted laminar features in EMOD (PPL); c) charcoal fragment in EMOD (PPL); d) iron segregations in the soil matrix of LROM1 (PPL); e) silty coatings around a pumice fragment, with internal iron segregations, in LROM1 (PPL); f) silty textural features in LROM3 (PPL); g and h) pore network filled by calcium carbonate segregations in PPL and XPL; i) weathered soil matrix in ENEO (PPL); l) iron segregations and clay coatings in MES (PPL).  
120x208mm (150 x 150 DPI)

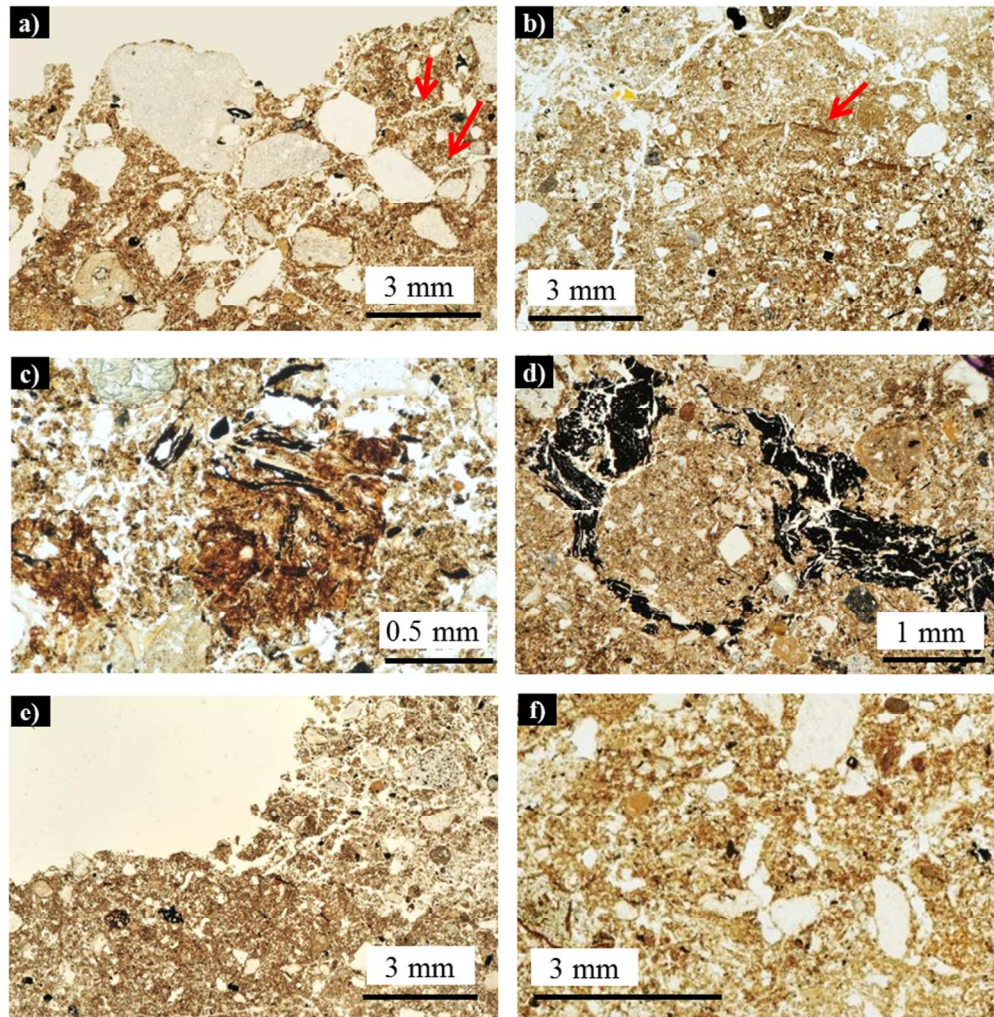


Figure 6. Micrographs of the Early Bronze Age microtopography in PPL. Microreliefs: a) crumb/granular structure in the first millimeters, where 2 red arrows indicated planar pores b) progressively massive structure with depth, with finer textured laminar aggregates horizontally oriented (indicated by the red arrow); c) organic residues mixed to charcoal in the soil matrix; d) fragment of strained charcoal embedded in the soil matrix; Microconcavity: e) massive and crumb structure on the surface, f) abundant fauna passages in depth.

159x162mm (150 x 150 DPI)



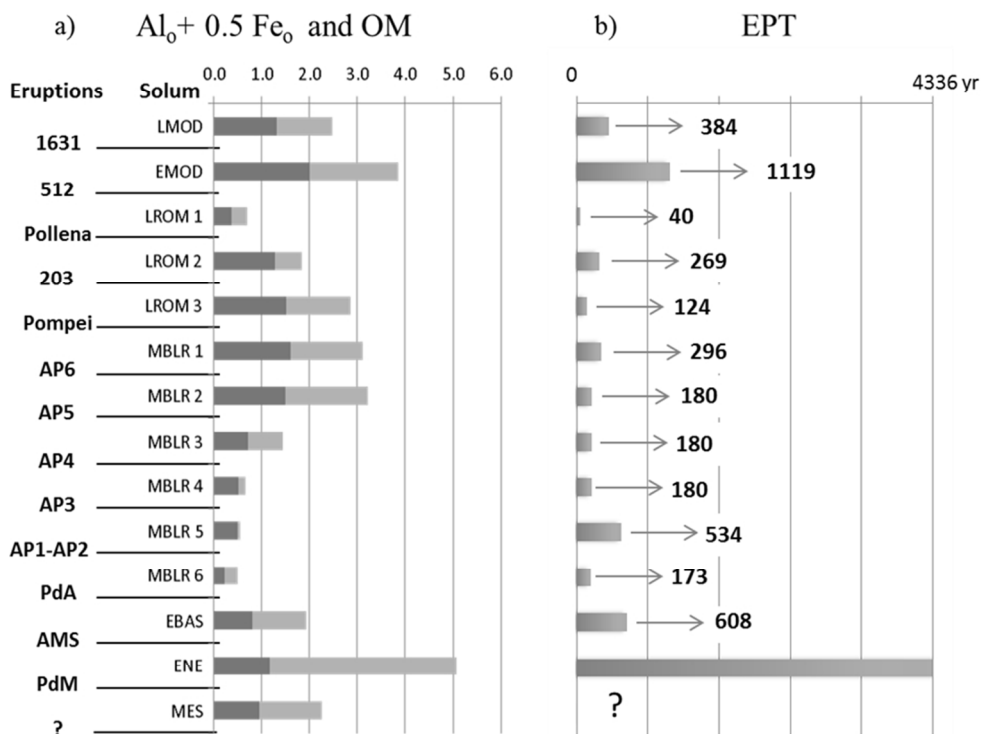


Figure 7. For each solum of the chronosequence are reported in a)  $Al_0+0.5Fe_0$  index (dark grey) and the OM (light grey), both in %; b) estimated pedogenetic times (EPT) in years.  
162x123mm (150 x 150 DPI)